NASA TECHNICAL MEMORANDUM

UB
NASA TM X-1583

UB
NASA TM X-1583

A PRELIMINARY FLYING-QUALITIES EVALUATION OF A VARIABLE-SWEEP FIGHTER-TYPE AIRCRAFT

by Thomas R. Sisk, Neil W. Matheny, David A. Kier, and John A. Manke

Flight Research Center
Edwards, Calif.

NATIONAL AERONAUTICS AND SPACE ADMINISTRATION • WASHINGTON, D. C. • MAY 1968

NASA TM X-1583

A PRELIMINARY FLYING-QUALITIES EVALUATION OF A VARIABLE-SWEEP FIGHTER-TYPE AIRCRAFT

By Thomas R. Sisk, Neil W. Matheny, David A. Kier, and John A. Manke

Flight Research Center
Edwards, Calif.

NATIONAL AERONAUTICS AND SPACE ADMINISTRATION

A PRELIMINARY FLYING-QUALITIES EVALUATION OF A VARIABLE-SWEEP FIGHTER-TYPE AIRCRAFT*

By Thomas R. Sisk, Neil W. Matheny, David A. Kier, and John A. Manke
Flight Research Center

SUMMARY

An evaluation of F-111A airplane number 6 (S/N 63-9771) consisting of 9 pilot-familiarization flights and 14 data-acquisition flights extending to Mach numbers approaching 1.9 at 47,500 feet (14,478 meters) altitude and 1.1 at 10,000 feet (3048 meters) altitude has been completed. This preliminary evaluation allowed the assessment of flight-control-system and airplane response characteristics at various wing sweeps over the normal operating envelope of the aircraft with stability augmentation on and off. Augmentation-off flight is considered to be outside the normal flight environment of an operational aircraft and to be an emergency condition.

With augmentation on, the longitudinal trim, maneuverability, and short-period dynamics, and the lateral-directional statics and Dutch roll dynamics were generally satisfactory over the Mach number range tested. The unaugmented longitudinal characteristics displayed high short-period frequencies at the higher dynamic pressures and high maneuvering force gradients over the supersonic speed range. Over the subsonic Mach number range at all wing sweeps, the airplane exhibited a mild pitch-up tendency that was masked by the augmentation system. Control effectiveness was high, and recovery from the pitch-up posed no problem. The pitch-up occurred simultaneously with the onset of buffet.

The augmented lateral-directional control system provided deadbeat damping of the Dutch roll oscillation; it did not, however, provide adequate roll response at rearward wing sweeps where the spoilers were inoperative. Adverse yaw was high and was most noticeable during the landing approach. The unaugmented lateral-directional characteristics displayed low Dutch roll damping at high dynamic pressures and large variations in dihedral effect throughout the test envelope.

The buffet-onset boundary for the 26° wing-sweep position decreased appreciably as the transonic region was approached. Increasing the sweep angle to 50° had a beneficial effect on buffet-onset conditions above an indicated Mach number of approximately 0.8. The buffet-onset normal-force coefficient for the 71.5° wing sweep was low and invariant throughout the subsonic Mach number range.

---

*Title, unclassified.

INTRODUCTION

F-111A airplane number 6 (S/N 63-9771) has been bailed to the NASA Flight Research Center for general research flight testing in the areas of stability and control, flight loads, structural temperatures, buffeting, and propulsion/performance as a continuation of NASA research on variable-sweep aircraft (ref. 1). Correlation of flight data derived from this program with theoretical predictions and ground-facility test results is expected to contribute significant background information toward the design and development of future variable-sweep military aircraft—FX, VFAX, AMSA—as well as the U. S. supersonic transport.

The initial portion of the Flight Research Center program consisted of an overall survey of airplane stability and control characteristics and handling qualities throughout the flight envelope. In order to make results available at an early date, the more significant results from this program are presented in this paper. More detailed results will be presented in later reports.

SYMBOLS

Because of changes in wing geometry with wing sweep, all parameters are based on the appropriate geometry.

a_l	longitudinal acceleration of center of gravity, g
a_n	normal acceleration of center of gravity, g
a_t	transverse acceleration of center of gravity, g
b	wing span, feet (meters)
C_{N_A}	airplane normal-force coefficient
F_a	aileron force at stick grip, pounds (newtons)
F_e	elevator force at stick grip, pounds (newtons)
F_p	pedal force, pounds (newtons)
g	acceleration due to gravity, 32.17 feet/second^2 (9.807 meters/second^2)
h_{p_i}	indicated pressure altitude, feet (meters)
K_p	adaptive roll gain, percent of maximum (1.0 degree/degree/second)

K_q	adaptive pitch gain, percent of maximum (1.25 degree/degree/second)
$\bar{L}$	rolling acceleration, per second^2
$\bar{L}_{\delta_a}$	roll-control-effectiveness parameter, $\frac{\partial \bar{L}}{\partial \delta_a}$ per second^2
$\bar{M}$	pitching acceleration, per second^2
M_i	indicated Mach number
$\bar{M}_{\delta_e}$	pitch-control-effectiveness parameter, $\frac{\partial \bar{M}}{\partial \delta_e}$ per second^2
P	period of short-period oscillation, seconds
p	rolling angular velocity, degrees/second
$\left(\frac{pb}{2V}\right)_{max}$	wing-tip helix angle for maximum roll rate, radians
q	pitching angular velocity, degrees/second
$\bar{q}$	dynamic pressure, pounds/foot^2 (newtons/meter^2)
r	yawing angular velocity, degrees/second
S	wing area, feet^2 (meters^2)
$T_{1/2}$	time to damp to one-half amplitude, seconds
t	time, seconds
V	true airspeed, feet/second (meters/second)
V_i	indicated airspeed, knots
$\frac{x_{cp}}{\bar{c}_{wp}}$	wing-panel chordwise center-of-pressure location, percent mean aerodynamic chord outboard of pivot
$\left(\frac{y_{cp}}{\frac{b}{2}}\right)_{wp}$	wing-panel spanwise center-of-pressure location, percent wing-panel semispan
α	angle of attack, degrees
β	angle of sideslip, degrees

δ_a	total aileron position, $\delta_{e_R} - \delta_{e_L}$, degrees
$\delta_{a_{servo}}$	aileron servo position, degrees
δ_e	elevator position, $\frac{\delta_{e_R} + \delta_{e_L}}{2}$, degrees
$\delta_{e_{servo}}$	elevator servo position, degrees
$\delta_{e_{tr_{series}}}$	elevator series trim position, degrees
δ_p	rudder-pedal position, inches (centimeters)
δ_r	rudder position, degrees
δ_{s_a}	aileron stick position at grip, inches (centimeters)
δ_{s_e}	elevator stick position at grip, inches (centimeters)
δ_{sp}	spoiler position, degrees
$\dot{\theta}$	pitching angular velocity, degrees/second
Λ	wing sweep at leading edge, degrees
φ	bank angle, degrees
$\dot{\psi}$	yawing angular velocity, degrees/second

Subscripts:

L	left
max	maximum
R	right

AIRPLANE DESCRIPTION

The F-111A is a two-place (side-by-side) long-range fighter bomber built by General Dynamics, Fort Worth Division. The airplane is designed for all-weather supersonic operation at both low and high altitude. Power is provided by two TF30-P-1 axial-flow, dual-compressor turbofan engines equipped with afterburners. The wings, equipped with leading-edge slats and trailing-edge flaps, may be varied in sweep angle

between 16° and 71.5°. The empennage consists of a fixed vertical stabilizer with rudder for directional control and a horizontal stabilizer (rolling tail) that is moved symmetrically for pitch control and asymmetrically for roll control. Wing spoilers augment roll-control power for wing-sweep angles of less than 47°. The main-landing-gear door acts as a speed brake.

The aircraft tested in this investigation was F-111A airplane number 6 (S/N 63-9771), a pre-SWIP (Super Weight Improvement Program) configuration. Although differences exist in the inertia characteristics and certain physical dimensions between airplane number 6 and SWIP aircraft, the results from these tests are believed to be generally representative of this class of variable-sweep aircraft.

Other features of the test aircraft include individual ejection seats, standard pre-SWIP engine inlet duct, translating inlet cowls, and production vortex generators in the inlet. The test aircraft does not have a low-speed trim compensator, an adverse yaw compensator, or inlet cone bleed.

A two-view drawing of the aircraft is shown in figure 1, and pertinent physical characteristics are listed in table I. Figure 2 shows the changes in wing geometry with wing-sweep angle, and figure 3 details the variable-geometry features of the wing. It should be pointed out that the flaps cannot be extended at wing sweeps greater than 26° and the total spoiler system is inoperative at sweep angles greater than 47°.

DESCRIPTION OF THE CONTROL SYSTEM

The F-111A flight control system incorporates pilot-assist modes, command augmentation (rate command) and adaptive-gain scheduling in pitch and roll, and a fixed-gain yaw damper. In pitch and roll, command augmentation and adaptive gains are designed to provide invariant aircraft response for pilot control throughout the operational envelope within the limits of control-system authority. A manual mode is available on the test aircraft that allows gains in pitch and roll to be selected manually. The gain levels are displayed on cockpit indicators.

The stability augmentation system utilizes standby redundancy in all axes. In the event of a failure in one of the three system channels, majority voting logic is used to isolate the malfunctioning channel and the operational status of the system is displayed to the pilot. Augmentation-off flight is considered to be outside the normal flight environment of an operational aircraft and to be an emergency condition.

Pitch Axis

A schematic drawing of the pitch axis and pertinent control characteristics are shown in figure 4(a). Primary pitch control is achieved by symmetrical movement of

the horizontal-tail surfaces through a mechanical-hydraulic system. With the control-system switch in the normal position and with augmentation on, stick position also commands a combination of pitch rate and normal acceleration which is fed electrically to the damper servo. The series trim actuator tends to keep the damper servo at a neutral position. At flight conditions where pitch rate is small, the series trim acts as an automatic trim which follows the acceleration feedback signal. Pitch adaptive gain is maintained at a desired level by sensing the damping of a high-frequency mode that is indicative of the system activity. An inverse model supplies second-order lead within an optimum region of the short-period aircraft dynamics to maintain deadbeat damping. The normal-acceleration signal and series trim are removed when the control-system switch is in the Takeoff/Land position.

Roll Axis

Roll control is obtained by differential movement of the horizontal stabilizer and spoilers. A schematic of this system is shown in figure 4(b). With augmentation off, one-half aileron stick displacement yields 4° total aileron and full stick displacement yields 15° total aileron. For wing sweeps of less than 45°, two sets of spoilers are deflected to their maximum of 43° with one-half stick displacement. For wing sweeps between 45° and 47°, the inboard spoilers on each wing are deactivated, and for wing sweeps greater than 47° the total spoiler control system is inoperative. The augmentation system commands roll rate as a function of stick position through the rolling tail only. With augmentation on, the maximum roll rate of 135 degrees/second is commanded within the maximum aileron authority of ±15° (total) at approximately one-half stick deflection (fig. 4(c)). At this stick deflection, a force detent (step increase) of approximately 7 pounds (31.14 newtons) is encountered. Optimum gain is maintained similar to the pitch control system.

Lateral trim is available only through the roll augmentation system.

Yaw Axis

Yaw control is obtained by a conventional rudder with control authorities of ±7.5° in the Normal mode or ±30° in the Takeoff/Land mode. The pilot can manually select 30° at any time. This system is illustrated in figure 4(d). The yaw augmentation system does not use the adaptive-gain feature. During normal flight, the sum of transverse acceleration and yawing angular rate positions the damper servo. This positioning circuit utilizes washout to reduce the rate signal during steady-state turns. In the Takeoff/Land mode, the washout circuit is removed and the yaw augmentation system senses transverse acceleration and one-third yawing angular rate.

INSTRUMENTATION

The test aircraft was equipped with conventional stability and control instrumentation, wing and horizontal-tail strain gages, and limited performance instrumentation.

The strain gages used for wing-panel loads are located at the pivot, and the horizontal-tail strain gages are located at the intersection of the torque tube and root

rib in each tail. Check loads performed prior to the flight program substantiated the contractor's calibration that was used for this evaluation.

A standard NASA airspeed head and angle-of-attack and angle-of-sideslip vanes are located on a 7.5-foot (2.29-meter) boom mounted on and ahead of the aircraft nose. The angle-of-attack and angle-of-sideslip parameters have not been corrected for the effects of angular rates, accelerations, or upwash. The angle of attack is measured relative to the fuselage reference line. Linear accelerometers are located on the rear weapons-bay bulkhead 2 feet (0.61 meter) to the right of the fuselage centerline and 4 to 5 feet (1.22 to 1.52 meters) ahead of the nominal center of gravity.

An airspeed calibration has not been completed on this installation; therefore, all Mach number and altitude data are presented in terms of indicated parameters.

All data in this paper are presented for the operational gross weight and corresponding center-of-gravity locations. The center-of-gravity location is referenced to the mean aerodynamic chord of the appropriate wing sweep (fig. 2). Aircraft weighing prior to the flight program established the gross-weight and center-of-gravity accuracies to be ±700 pounds (±317.5 kilograms) and ±1.7 inches (±4.32 centimeters), respectively.

The data-acquisition system used was pulse code modulation (PCM) and provided onboard recording and telemetry.

TEST PROGRAM

The evaluation consisted of 9 pilot-familiarization flights and 14 data-acquisition flights that extended to Mach numbers approaching 1.9 at 47,500 feet (14,478 meters) altitude and 1.1 at 10,000 feet (3048 meters) altitude. Specific maneuvers designed to evaluate the stability and control characteristics, buffeting, and wing/tail load levels were performed at selected flight conditions throughout the flight envelope, including an arbitrary climb corridor (fig. 5). In general, all maneuvers were performed with stability augmentation on and off to permit assessment of the unaugmented aircraft characteristics as well as the contribution provided by various augmentation elements. Takeoff/climbout and approach/landing characteristics as well as level-flight accelerations and ground handling were evaluated during the testing.

Maximum internal fuel was loaded for each flight; however, maneuvers were not initiated until the integral wing tanks were empty. All testing was at center-of-gravity locations controlled by the automatic fuel-sequencing system (i.e., with the engine feed selector switch in Automatic).

RESULTS AND DISCUSSION

Summary of Control-System Characteristics

As stated earlier, the F-111 control system has command augmentation and adaptive-gain scheduling. Since these features play an important role relative to the

pilot's opinion of the handling qualities and, in some cases, actual airplane response characteristics, pertinent operational characteristics of the system will be reviewed before the aircraft flying qualities are discussed.

Longitudinal-system characteristics. – In general, the longitudinal stability augmentation system provides reasonable force gradients during takeoff. Figure 6(a) is a time history of a typical takeoff performed early in the program and illustrates the most significant characteristics. The rate-command system requires that back pressure on the stick be released to prevent overrotation. This does not present any particular problem, although it might surprise a pilot not familiar with rate-command systems and may necessitate a significant push force after lift-off. There is little or no trim change with gear retraction. However, a rapid nose-down input is required by the pilot to counter the nose-up pitching transient associated with retraction of the flaps from full down to the loiter position. The inability of the augmentation system to mask this trim change probably stems from the rapid rate of flap travel.

Another feature of the rate-command system that may cause the pilot occasional difficulty during the landing approach is the apparent lack of speed stability. In a rate-command system, stick position maintains pitch rate rather than angle of attack. If, on a high final approach, the pilot pushes forward on the stick momentarily to increase the rate of descent and then returns the stick to neutral to regain the original attitude, the aircraft will maintain the new pitch angle and rate of sink, since the zero stick position is commanding zero pitch rate. This would increase the sink rate beyond that desired by the pilot and, if performed too close to the ground, could result in a dangerously high sink rate at touchdown and an undershoot of the intended touchdown point. It is believed that this characteristic may be the so-called "negative ground effect" mentioned by a number of pilots.

The trim change associated with wing sweep is hardly noticeable to the pilot with pitch augmentation engaged. This is illustrated in figure 6(b), which shows the effects of a wing-sweep change from 16° to 71.5°. It is seen that no significant stick inputs were required by the pilot as the trim angle of attack increased from 2.5° to 9°. The system functions well as an automatic trim, as illustrated in figure 6(c) for a constant-altitude acceleration.

The command augmentation system also maintains the maneuvering stick-force gradient within a range acceptable to the pilot throughout the flight range tested. Figure 6(d) shows that the gradient increases from approximately 6 lb/g to 12 lb/g (26.7 N/g to 53.4 N/g) as the Mach number increases from 0.7 to 1.83 along the arbitrary climb corridor shown in figure 5.

Lateral-system characteristics. – Structural limitations precluded the performance of abrupt rolls; instead, rapid 45° to 45° bank free-hand rolls were performed using stick deflections to the stick-force detent [approximately one-half aileron stick deflection (fig. 4(c))]. One-half stick deflection yields 4° total aileron with roll augmentation off, a maximum of 15° total aileron with augmentation on, and full deflection of the spoilers (for $\Lambda < 47°$) with augmentation off or on. (The spoilers are not activated through the augmentation system.) Therefore, even with minimum gain settings of the adaptive system, a significant increase in roll power is realized with roll-augmentation activation. This increase is illustrated in figure 7(a), which presents time histories of three aileron rolls at an indicated Mach number of 0.72 and an altitude of

20,500 feet (6248 meters). These rolls were performed with a wing sweep of 50°; consequently, the spoilers were inoperative. As shown, the total aileron deflection increased from 4° to 15° with an attendant roll-rate increase from 13 deg/sec to 57 deg/sec when the roll augmentation was activated. When the gain was set manually at 20 percent, the servo input was relatively slow, taking approximately 1 second to achieve maximum roll rate. Data are also shown for a roll with the gain adjusted to 100 percent. The time history indicates that the servo input was sufficiently rapid to allow the peak roll rate to be reached in approximately 0.5 second.

Increases in roll rate above the values in figure 7(a), as with spoiler activation, uncover a system characteristic that limits roll performance. With increased response, the augmentation system tends to reduce the aileron servo input before the commanded roll rate is attained. A time history of an aileron roll illustrating this characteristic is shown in figure 7(b). The wing sweep for this roll was 45° (instead of 50°, as in figure 7(a)) to allow spoiler operation and, consequently, higher roll rates. The reduction in aileron servo input begins shortly after time 0.4 second when the roll rate had reached a value of approximately 60 degrees/second.

Because of the nature of the rate-command system, the aircraft is spirally stable with the roll augmentation on. However, the spiral motion was divergent with augmentation off but was difficult to assess because of the inability to trim the aircraft laterally.

Adaptive-gain characteristics. – Buffeting, atmospheric turbulence, and excessive pilot control action all tend to drive the system gains down. Figure 8(a) is a time history of the pitch and roll gain response during a windup turn at an indicated Mach number of 0.70 and 25,000 feet (7620 meters) altitude with a wing sweep of 26° in which moderate-to-heavy buffeting was encountered. This time history shows a reduction of almost 50 percent in pitch and roll gains in the time it took to perform the maneuver. Figure 8(b) summarizes gain activity from all causes as a function of the control-effectiveness parameters for pitch and roll. The solid line represents the estimated decrease in normal gain level with increased control effectiveness, and the symbols present flight data based on control-effectiveness derivatives predicted by the contractor.

Airplane Response Characteristics

Longitudinal maneuverability. – It has been noted that, with pitch augmentation on, the takeoff force gradients are reasonable (fig. 6(a)) and the maneuvering stick-force gradient is maintained within a range acceptable to the pilot throughout the flight range tested (fig. 6(d)). With the pitch damper off, however, the takeoff is characterized by high stick force for rotation and noticeably large trim changes with actuation of the flaps and wing sweep, and the maneuvering stick-force gradient is found to be excessive in the high subsonic and supersonic portion of the flight envelope. The maneuvering force gradients along the arbitrary climb corridor are summarized in figure 9. As shown, the gradient approaches 30 lb/g (133.5 N/g) at the higher supersonic speeds. As in figure 6(d), these data have not been corrected to constant gross weight and center of gravity. Figure 9 also indicates that the supersonic maneuver capability will be limited by available control deflections to between 2 and 3 incremental g, depending on the 1-g trim requirement.

A mild stick-fixed instability (pitch-up) occurred throughout the subsonic Mach number range at all wing sweeps. Figure 10(a) presents two windup-turn crossplots for an indicated Mach number of 0.92 and 28,000 feet (8534 meters) altitude at the 50° wing-sweep position. The left side of the figure shows data obtained with the pitch damper on and the right side, with the damper off. The right-hand plot shows the instability to occur at an angle of attack of approximately 8° ($a_n \approx 2g$). It is apparent that the instability is masked with the pitch damper engaged. A comparison of the stick force per g for these two maneuvers illustrates the large reduction in this gradient produced by the pitch damper.

Longitudinal-control effectiveness is excellent for all conditions tested, and recovery from the pitch-up poses no problem. The rapid airplane response to the longitudinal control as the pilot "feels out" the airplane in the pitch-up region is illustrated in the time history of figure 10(b).

Pitch-up occurred simultaneously with buffet onset (discussed later), as determined from data obtained from a normal accelerometer at the aircraft center of gravity. Analysis of the wing-panel center-of-pressure data for this maneuver (fig. 10(c)) shows a movement forward and inboard at angles of attack above 8°, which indicates wing-tip flow separation.

A recovery of the apparent stability has been noted at angles of attack above that for pitch-up for the forward wing sweeps. This effect is illustrated in figure 11, which presents the results of a windup turn at an indicated Mach number of 0.79 and 25,700 feet (7833 meters) altitude. This maneuver was performed with 26° of wing sweep and with the pitch damper on. The pitch-up occurs at an angle of attack near 4° ($a_n \approx 1.5$ g) followed by an apparent increase in stability above approximately 7° angle of attack. As indicated by model tests (ref. 2), this apparent increase is probably due to flow separation at the wing—glove juncture. The increased slope of the α/g curve above 7° angle of attack also indicates that additional flow separation has occurred.

Dihedral effect. – Airplane dihedral effect was found to be positive and was reported by the pilot to vary greatly with Mach number and wing sweep. The smallest dihedral effect (near zero) was observed in the transonic speed range with forward wing sweeps, whereas the largest dihedral effect occurred at supersonic speeds and rearward wing sweeps. Although masked by the lateral augmentation system, the larger values of roll-due-to-sideslip for the unaugmented airplane significantly degraded the pilot's opinion of the handling qualities. The significance of the increased dihedral effect is illustrated in figure 12, a time history of a rudder-induced lateral-directional maneuver at 71.5° wing sweep with roll and yaw augmentation off. Superimposed on this figure is a portion of a full-deflection aileron roll at approximately the same flight condition with augmentation on. A comparison of these two time histories shows that although initial aircraft roll response to the rudder lagged the control input by almost 1 second, the roll rates obtained by using either the rudder with dampers off or ailerons with dampers on were of the same order. According to the pilot, this characteristic would make roll-damper-off operation at the higher dynamic pressures in the presence of atmospheric turbulence extremely hazardous.

Lateral maneuverability. – As might be expected, minimum roll rates occur just after spoiler deactivation at approximately 50° wing sweep. The time histories in

figure 13(a) of two rolls at $M_i = 0.71$ and 20,000 feet (6096 meters) altitude with dampers on illustrate the roll power of the spoilers. It may be seen that the rolling tail alone generates a peak roll rate of approximately 60 degrees/second, whereas, with the spoilers operative, the peak rate approaches 105 degrees/second. To re-emphasize two points made earlier, note that: (1) the roll response with spoilers operative lags the response with spoilers inoperative by as much as 10 degrees/second early in the maneuver because of the 20-percent lower gain setting, and (2) the peak roll rate would have been higher than 105 degrees/second had the aileron servo not started reducing the aileron deflection at a roll rate of approximately 80 degrees/second.

Figure 13(b) summarizes the aircraft roll response as a function of wing-sweep position at one flight condition ($M_i = 0.71$ at 20,000 feet (6096 meters) altitude). The data are adjusted to 15° total aileron deflection (or 135 degrees/second roll rate if 15° yielded greater than design roll response), and the helix-angle calculation is based on the span corresponding to the appropriate wing-sweep angle (fig. 2). Figure 13(b) illustrates the reduction in the rolling power of the spoilers as the wings are swept rearward and the loss in rolling power when the spoilers are inoperative. The reduction in roll inertia and damping in roll with increased wing sweep probably accounts for the slight increase in the bank angle attained in 1 second for wing sweeps greater than 50°.

The level of adverse yaw generated during the rolls, as illustrated in the aileron roll time history of figure 12, is summarized in the bottom curve of figure 13(b). All rolls were performed with the yaw damper on to minimize yaw effects on roll performance. Subsequent analysis of the data, however, has shown that the yaw damper actually degrades roll performance slightly by initiating rudder commands in response to favorable yawing rates (the "washout" circuit has reduced the rudder input from the steady-state left-yaw rate), as shown in the aileron-roll time history of figure 12. As noted earlier, the test aircraft was not equipped with an adverse yaw compensator.

Adverse yaw, according to the pilot, is present to some degree throughout the flight envelope regardless of whether augmentation is on or off. With augmentation off, however, the directional oscillations couple with the roll mode, making it very difficult to perform precise tracking maneuvers. This is particularly noticeable in the augmentation-off landing maneuver when the pilot must wait up to 10 seconds to determine the adequacy of heading corrections because of the rather poor Dutch roll damping characteristics in the landing configuration ($\Lambda = 26°$) and flight condition. An additional disconcerting factor stems from the fact that the magnitude of the generated sideslip is not readily apparent, and the side forces are too low to provide suitable cues to the pilot.

Short-period dynamics. – The augmented airplane shows essentially deadbeat damping of the longitudinal short-period and Dutch roll oscillations throughout the flight envelope tested. With augmentation off at the highest dynamic pressures experienced, however, the longitudinal short-period frequency becomes high (tending to excite pilot-induced oscillations (PIO)) and the Dutch roll damping becomes low. These trends are illustrated in figures 14(a) and 14(b), which present data obtained during two flights to an indicated Mach number of 1.1 at 10,000 feet (3048 meters) altitude. The first of these flights was made in severe turbulence, and the pilot reported that extreme caution had to be exercised to prevent PIO's in the pitch axis. Also, the Dutch roll oscillation became so large and persistent that he decided against

disengaging the augmentation at the 71.5° wing-sweep position at a Mach number of 1.1. The second flight was accomplished in smooth-air conditions. In comparing the two flights, the pilot reported that turbulence degrades handling qualities between two and three numbers on the Cooper Rating Scale at these flight conditions.

Airplane Buffet Characteristics

Data defining the airplane buffet characteristics were obtained at wing-sweep positions of 26°, 50°, and 71.5°. Buffet onset was identified from normal-accelerometer data as the point at which a definite oscillation (approximately ±0.02g) was visible on the trace.

Buffet-onset boundaries for the three wing-sweep positions are presented in figure 15 as a function of airplane normal-force coefficient and angle of attack. The buffet-onset boundary for the 26° sweep position decreases appreciably as the transonic region is approached. Increasing the sweep angle to 50° has a beneficial effect on buffet-onset conditions above $M_i \approx 0.8$. The buffet-onset normal-force coefficient for the 71.5° wing-sweep position is low and invariant throughout the subsonic Mach number range. (The airplane normal-force coefficient for buffet onset is based on the wing area corresponding to the appropriate sweep angle (fig. 2), and care must be taken when comparing wing-sweep buffet levels.)

Pilot reports of buffet onset correlated closely with accelerometer data. The pilot reported that the buffet intensity increased with increasing angle of attack up to a certain level and then, in most cases, remained essentially constant as angle of attack was increased further. This feature precludes using buffet for stall warning and points out the possible need for a stall preventative or warning device.

As noted in figure 15, a mild buffet-type vibration occurred supersonically with 71.5° wing sweep, but the pilot reported no significant increase in intensity with increasing angle of attack.

CONCLUDING REMARKS

A preliminary evaluation of the flying qualities of a pre-SWIP F-111A airplane (S/N 63-9771) was performed with stability augmentation on and off. Augmentation-off flight is considered to be outside the normal flight environment of an operational aircraft and to be an emergency condition.

The augmented longitudinal control system compensated for most aircraft configuration trim changes and, over the Mach number range investigated, functioned well as an automatic trim, maintained essentially constant maneuvering force gradients, and provided deadbeat damping for the short-period oscillation.

With augmentation off, takeoff was characterized by high stick force for rotation and large trim changes with flap actuation and wing sweep. Maneuvering stick-force gradients became high at the higher supersonic speeds, and longitudinal short-period frequencies became high (with attendant pilot-induced-oscillation tendencies) at the

highest dynamic pressures tested. The airplane exhibited a mild pitch-up tendency over the subsonic Mach number range at all wing sweeps that was masked from the pilot by the longitudinal augmentation system. Control effectiveness was high, and recovery from the pitch-up posed no problem. The pitch-up occurred simultaneously with buffet onset. A recovery in the apparent stability occurred at angles of attack above buffet onset for forward wing-sweep positions.

With augmentation on the lateral-directional statics and Dutch roll dynamics were generally satisfactory over the Mach number range tested. The dihedral effect was positive and varied from near zero in the transonic speed range and forward wing sweeps to extremely high values at supersonic speeds and rearward wing sweeps. The high dihedral effect had an adverse effect on the handling qualities when the airplane was in atmospheric turbulence with the roll augmentation off. Roll control power was reduced appreciably at the rearward wing sweeps where the spoilers were inoperative.

Adverse yaw was present to some extent throughout the flight envelope regardless of whether augmentation was on or off and was most noticeable during the landing approach. The Dutch roll damping, with augmentation off, became low at the highest dynamic pressures tested.

The boundary for buffet onset for the 26° wing-sweep position decreased appreciably as the transonic region was approached. Increasing the sweep angle to 50° had a beneficial effect on buffet-onset conditions above an indicated Mach number of approximately 0.8. The buffet-onset normal-force coefficient for 71.5° wing sweep was low and nonvarying throughout the subsonic Mach number range.

Flight Research Center,
National Aeronautics and Space Administration,
Edwards, Calif., March 13, 1968,
720-06-00-02-24.

REFERENCES

1. Spearman, M. Leroy; and Foster, Gerald V.: A Summary of Research on Variable-Sweep Fighter Airplanes. NASA TM X-1185, 1965.

2. Boisseau, Peter C.: Flight Investigation of Dynamic Stability and Control Characteristics of a 1/10-Scale Model of a Variable-Wing-Sweep Fighter Airplane Configuration. NASA TM X-1367, 1967.

TABLE I. – PHYSICAL CHARACTERISTICS OF THE F-111A AIRPLANE (NUMBER 6)

Wing –	
Airfoil section, at pivot	NACA 64A210.7 (modified)*
Airfoil section, tip	NACA 64A209.8 (modified)*
Sweep, degrees (leading edge)	16 to 71.5
Incidence, deg	1
Dihedral, deg	1
Span, area, mean aerodynamic chord	(See fig. 2)
Leading-edge slats –	
Area (planform projected), ft^2 (m^2)	48.5 (4.38)
Span, percent of exposed wing-panel span	96.5
Deflection, maximum, deg	45
Trailing-edge flaps –	
Type	Multisection Fowler
Area (aft of hinge line), ft^2 (m^2)	108 (9.75)
Span, percent of exposed wing-panel span	100
Deflection, maximum, deg	35
Spoilers –	
Area (planform projected), ft^2 (m^2)	30.3 (2.74)
Span, ft (m)	11.8 (3.6)
Deflection, maximum, deg	43
Wing pivot –	
Distance from airplane nose, ft (m)	38.80 (11.83)
Distance from airplane centerline, ft (m)	5.86 (1.79)
Horizontal tail (all movable) –	
Airfoil section	BICONVEX
Incidence, deg	1
Dihedral, deg	-1
Sweep at leading edge, deg	57.5
Span, ft (m)	29.9 (9.11)
Area (exposed), ft^2 (m^2)	174.3 (15.74)
Area (movable), ft^2 (m^2)	154.2 (13.92)
Aspect ratio	1.54
Mean aerodynamic chord (exposed), in. (cm)	137.5 (349.3)
Deflection, maximum, deg:	
As elevators:	
Trailing-edge up	(approx.) 25
Trailing-edge down	(approx.) 10
As ailerons (total)	(approx.) ±15
Surface stops:	
Trailing-edge up	(approx.) 31
Trailing-edge down	(approx.) 16
Vertical tail –	
Airfoil section	BICONVEX
Sweep at leading edge, deg	55
Span, ft (m)	8.9 (2.71)
Area, ft^2 (m^2)	111.7 (10.09)
Aspect ratio	1.42
Mean aerodynamic chord, in. (cm)	159.3 (404.6)
Rudder –	
Span, ft (m)	7.8 (2.38)
Area, ft^2 (m^2)	29.3 (2.65)
Deflection, maximum, deg	±30
Speed brake –	
Area, ft^2 (m^2)	26.5 (2.39)
Deflection, maximum, deg	77
Ventrals –	
Area (total), ft^2 (m^2)	25 (2.26)
Power plants –	
P & W TF30-P-1 engines	2

*Unswept wing.

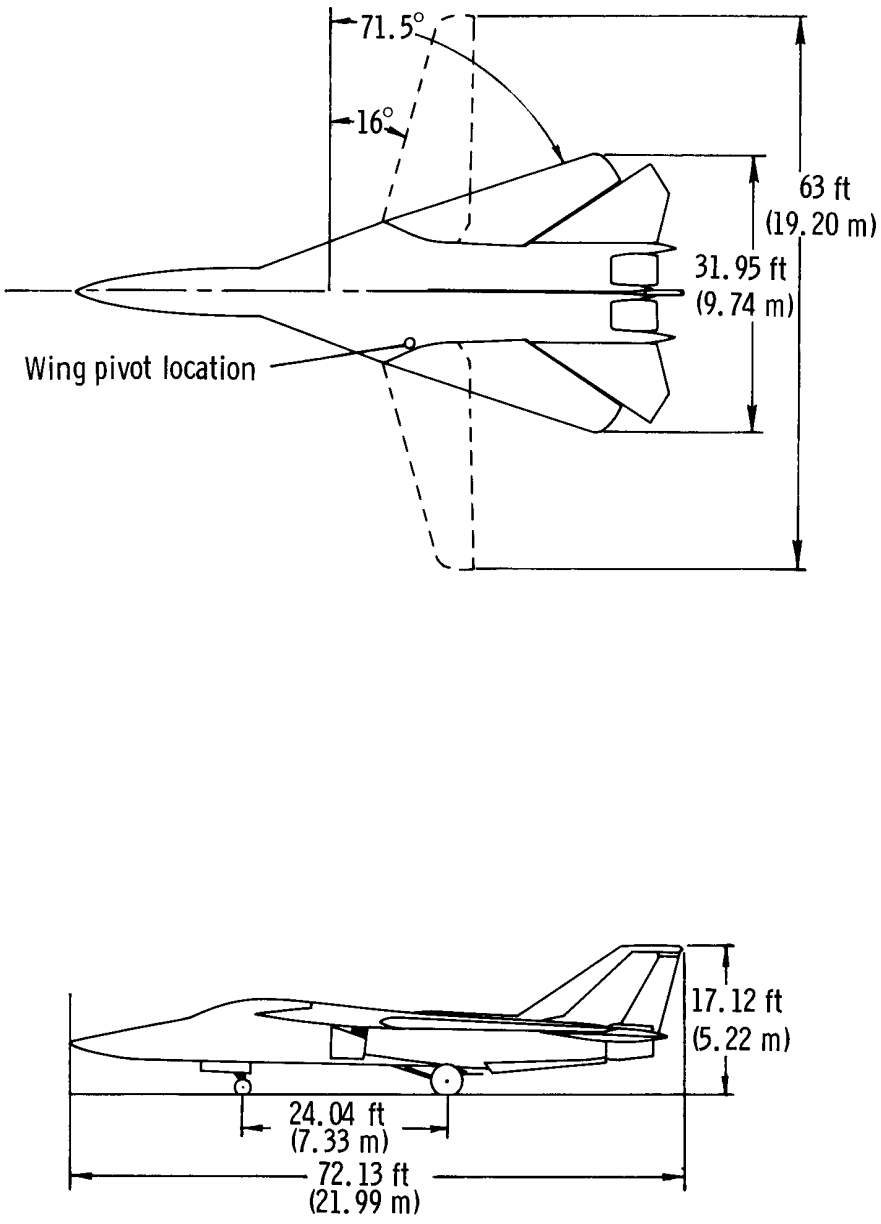

Figure 1. – Two-view drawing of F-111A airplane. Pre-SWIP configuration.

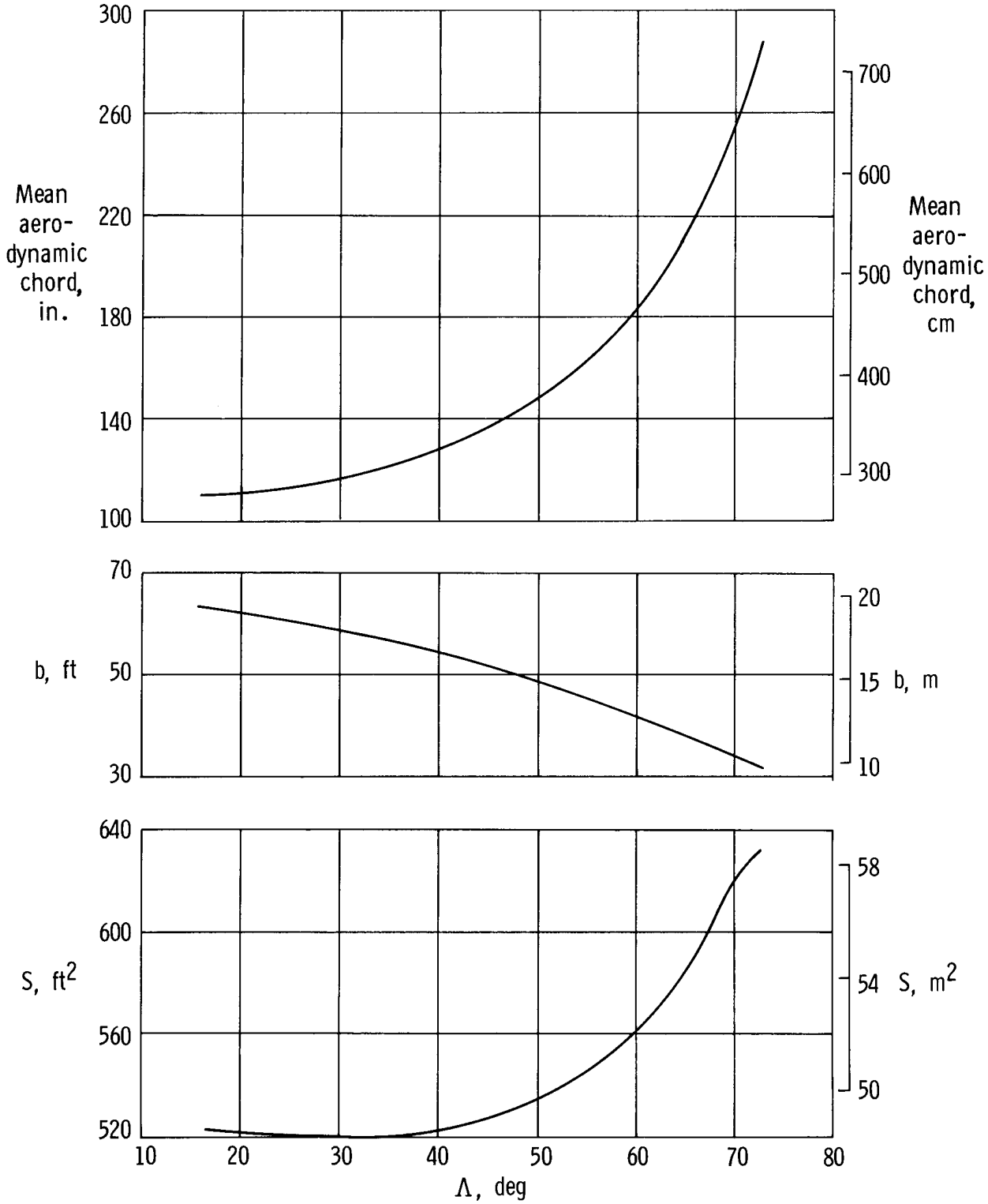

Figure 2. – F-111A wing geometry as a function of wing sweep.

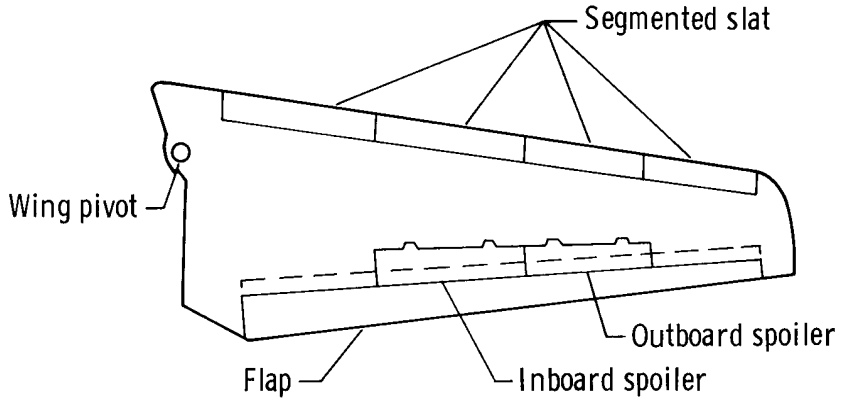

(a) Wing planform.

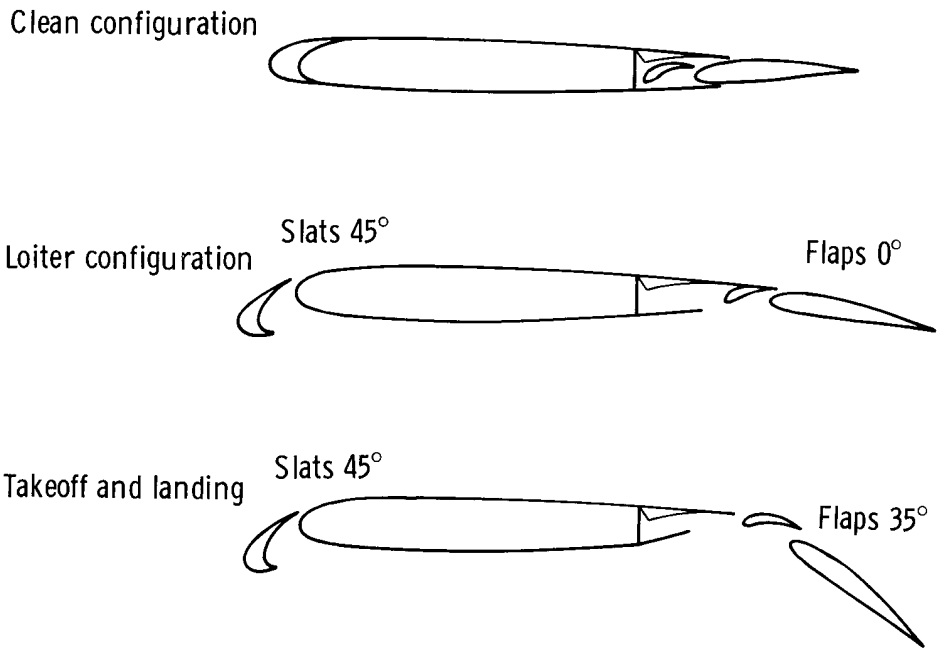

(b) Flap/slat details.

Figure 3. – Details of F-111A wing.

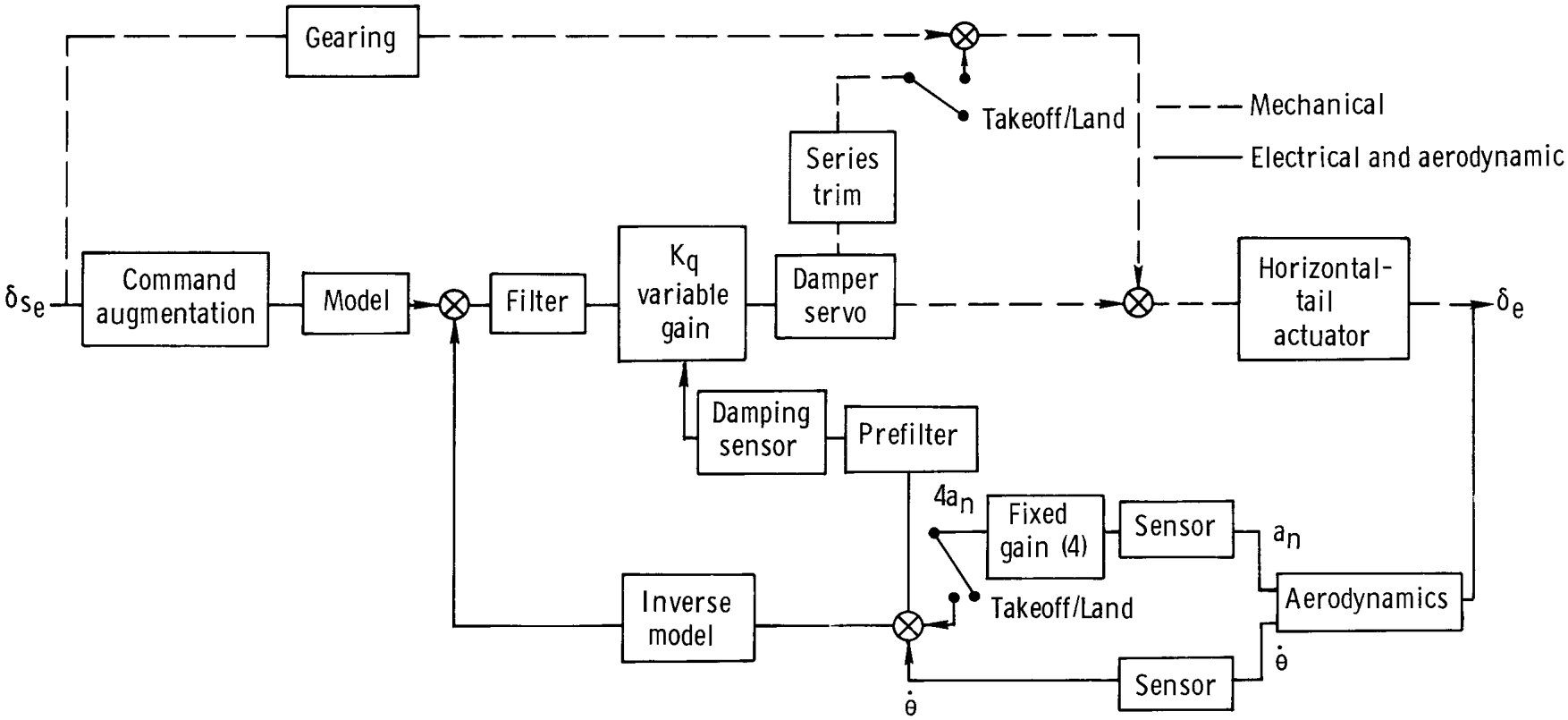

	Control stick	Damper	Series trim	Elevator
Travel or authority	Aft 7.0 in. (17.78 cm) Forward 2.8 in. (7.11 cm)	±12°	10° trailing edge up 4° trailing edge down	25° trailing edge up 10° trailing edge down
Maximum rate (design)	----------	84 deg/sec	1.4 deg/sec	36 deg/sec

(a) Pitch-axis schematic.

Figure 4. – F-111A control system (airplane number 6).

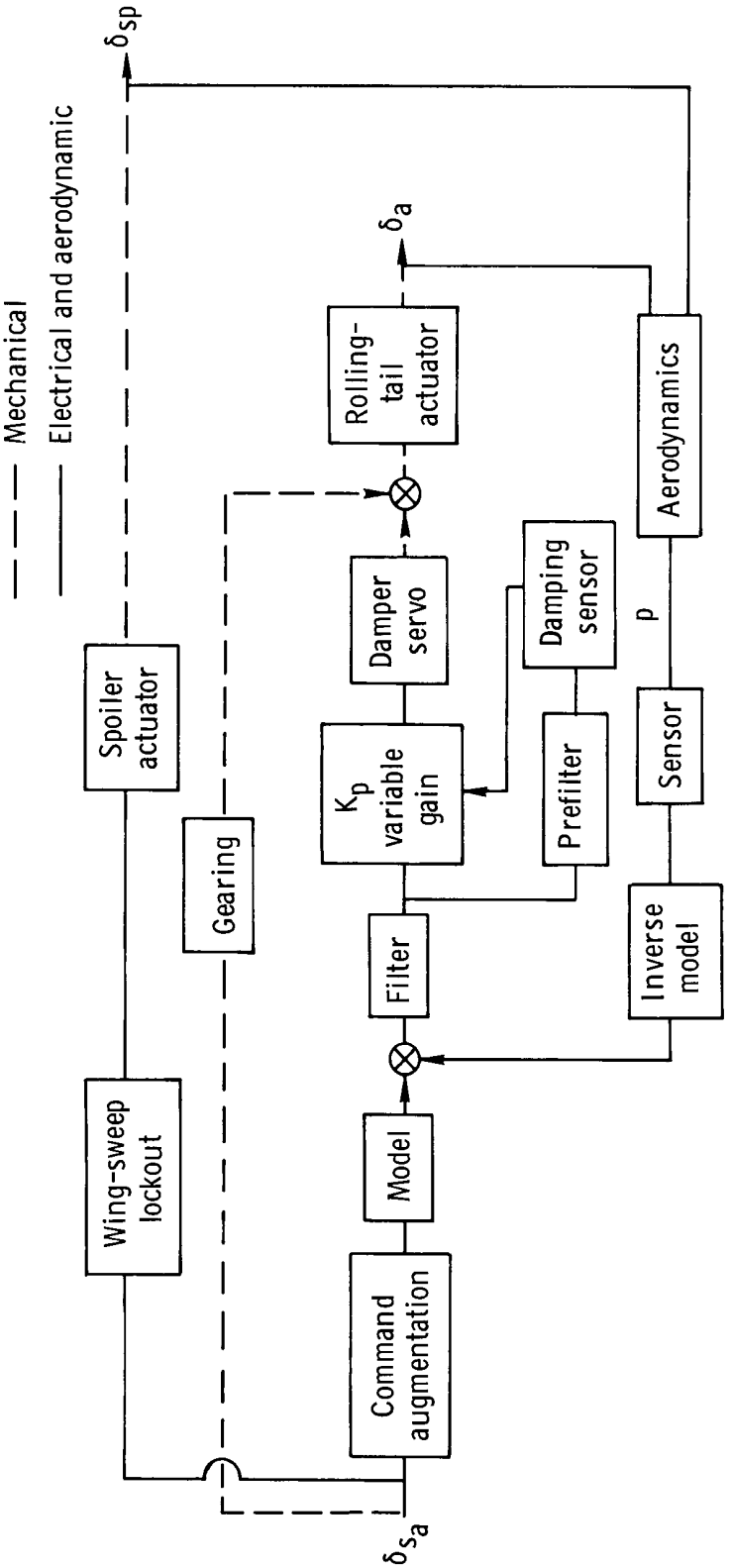

	Stick	Damper	Aileron	Spoiler
Travel or authority	±4.75 in. (12.07 cm)	±11° (total)	±15° (total)	43°
Maximum rate (design)	----------	84 deg/sec	36 deg/sec	170 deg/sec

(b) Roll-axis schematic.

Figure 4. – Continued.

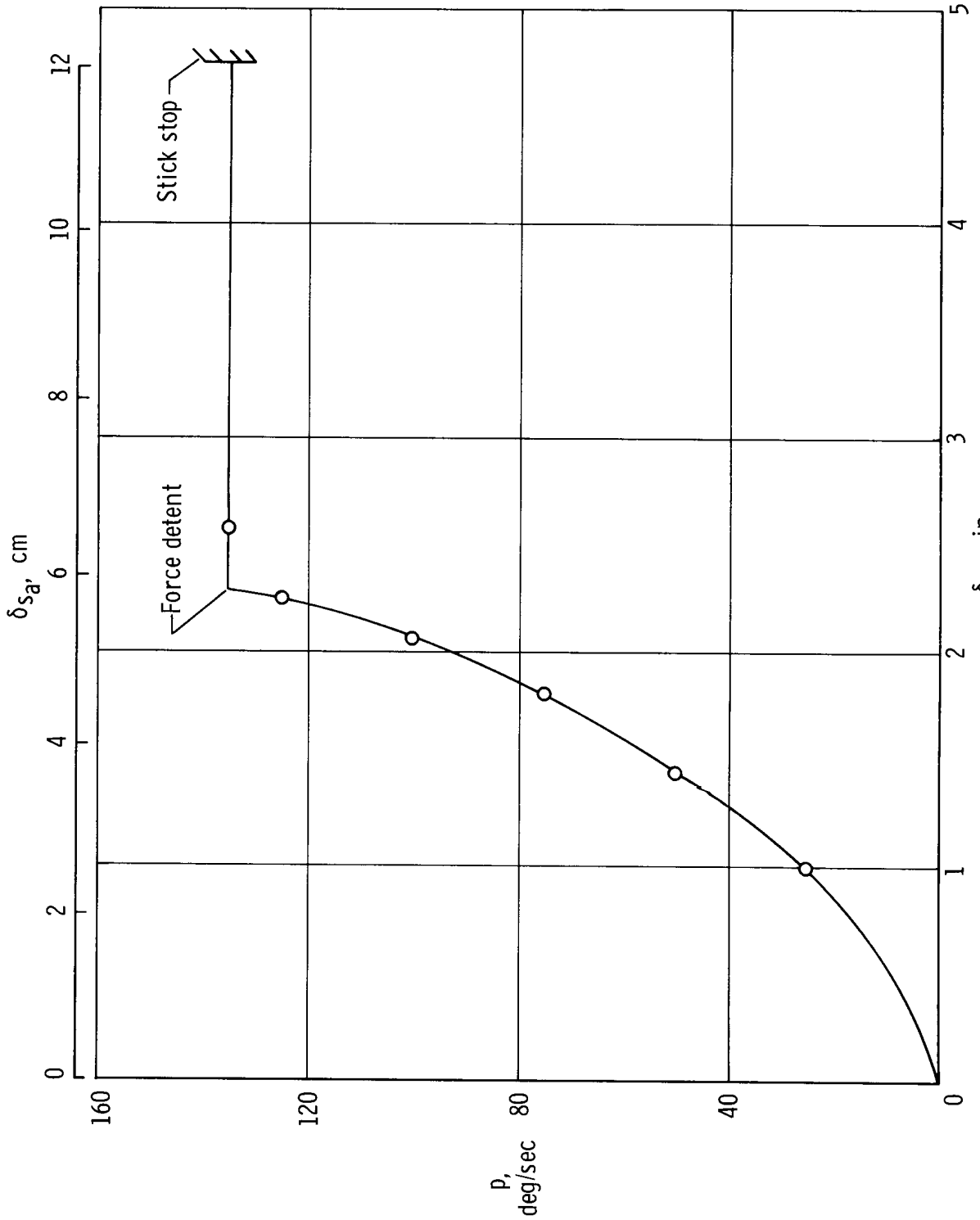

(c) Roll rate command schedule. Ground test data with augmentation on.

Figure 4. – Continued.

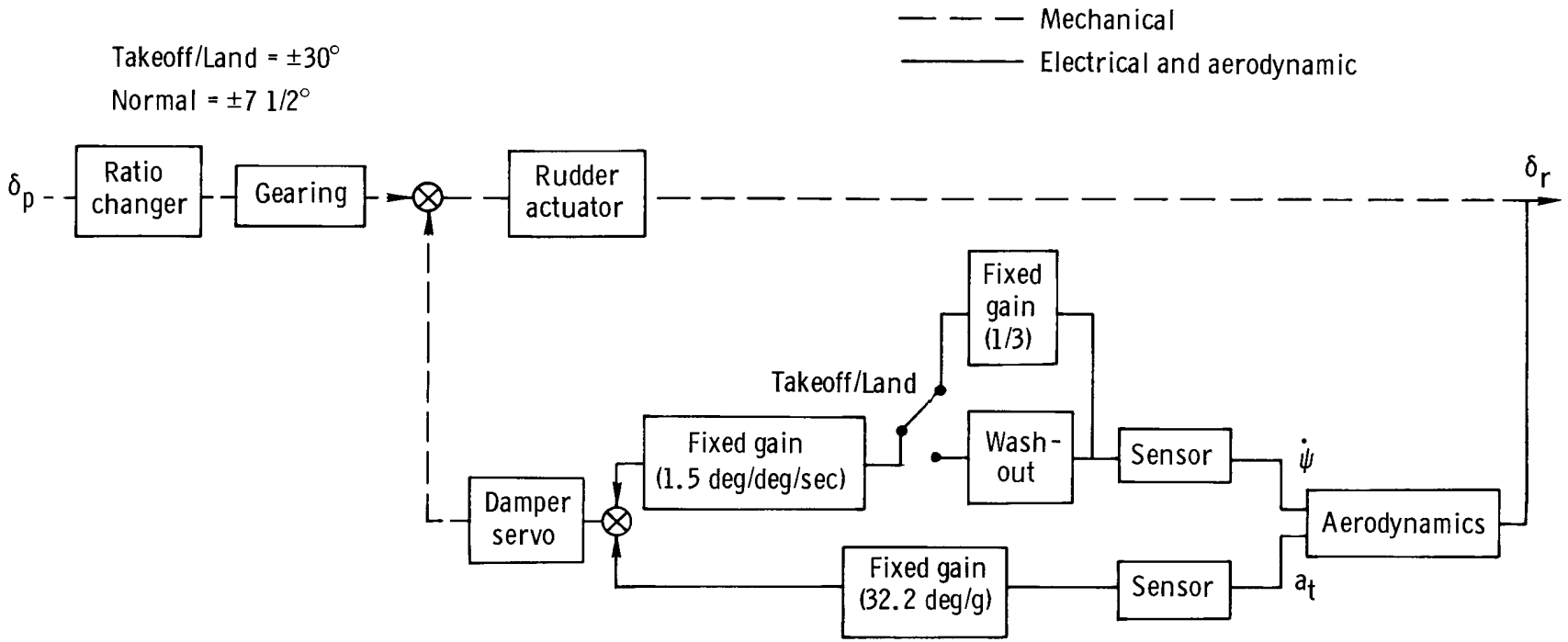

	Pedal	Damper	Rudder
Travel or authority	±3 in. (7.62 cm)	±5°	±30° or ±7.5° selected by control-system switch
Maximum rate (design)	----------	35 deg/sec	160 deg/sec

(d) Yaw-axis schematic.

Figure 4. – Concluded.

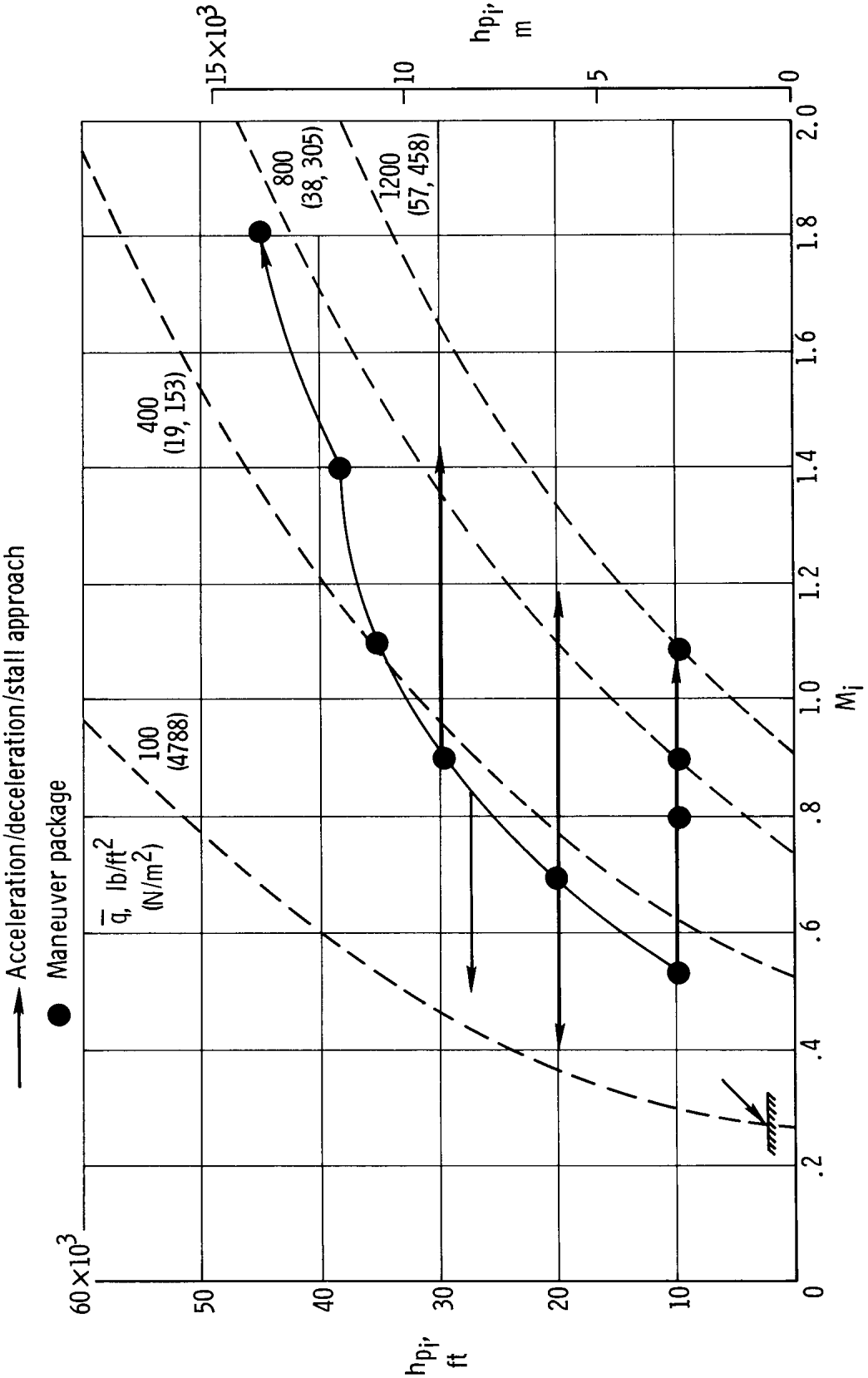

Figure 5. – F-111A test program Mach number and altitude coverage.

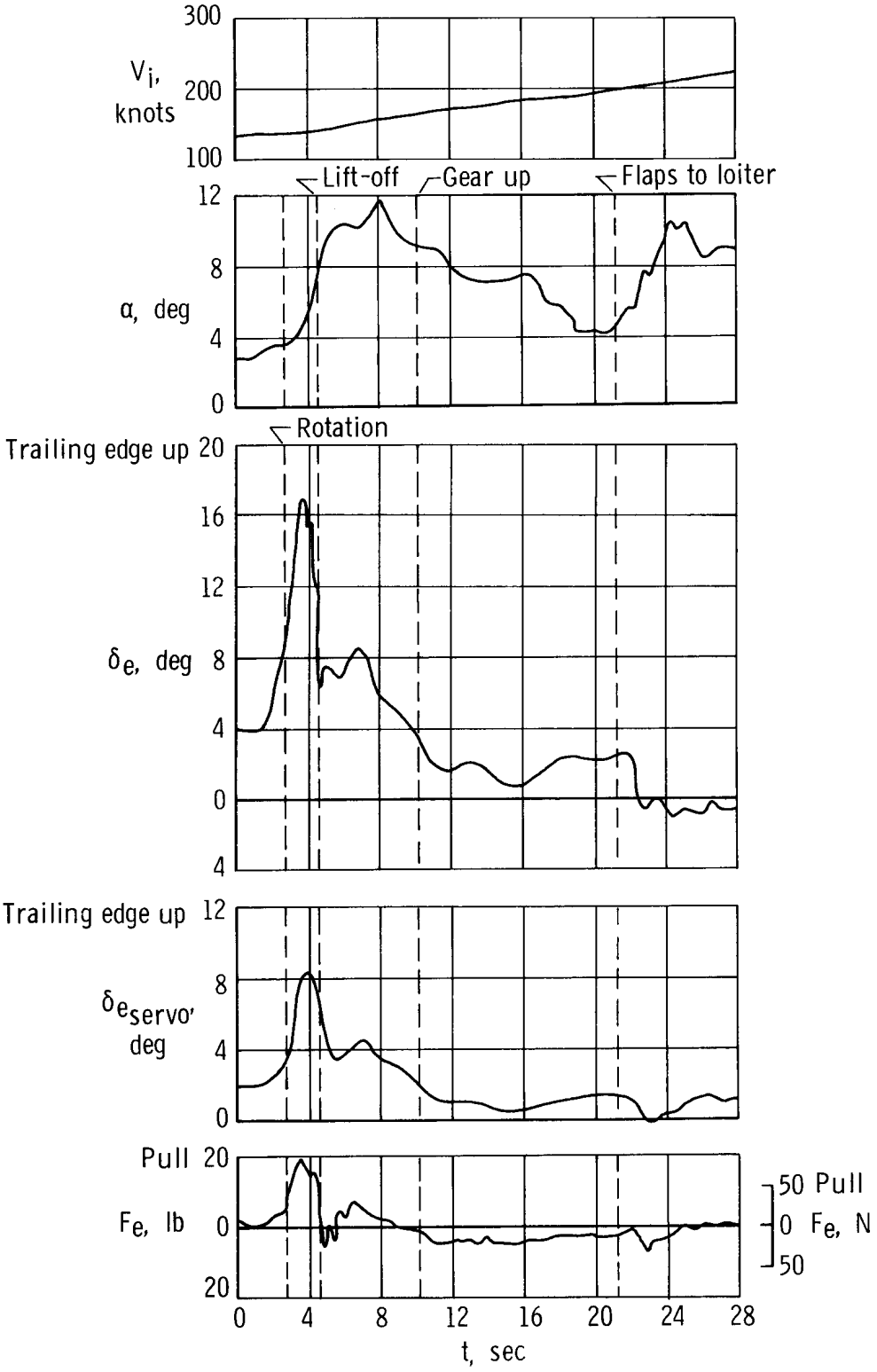

(a) Trim changes during maximum afterburner takeoff with full flaps. Λ = 16°; gross weight = 77,000 lb (34,800 kg); center of gravity = 29.5 percent; $\delta_{e_{tr_{series}}}$ = 3.5° trailing edge up.

Figure 6. – F-111A longitudinal command augmentation characteristics.

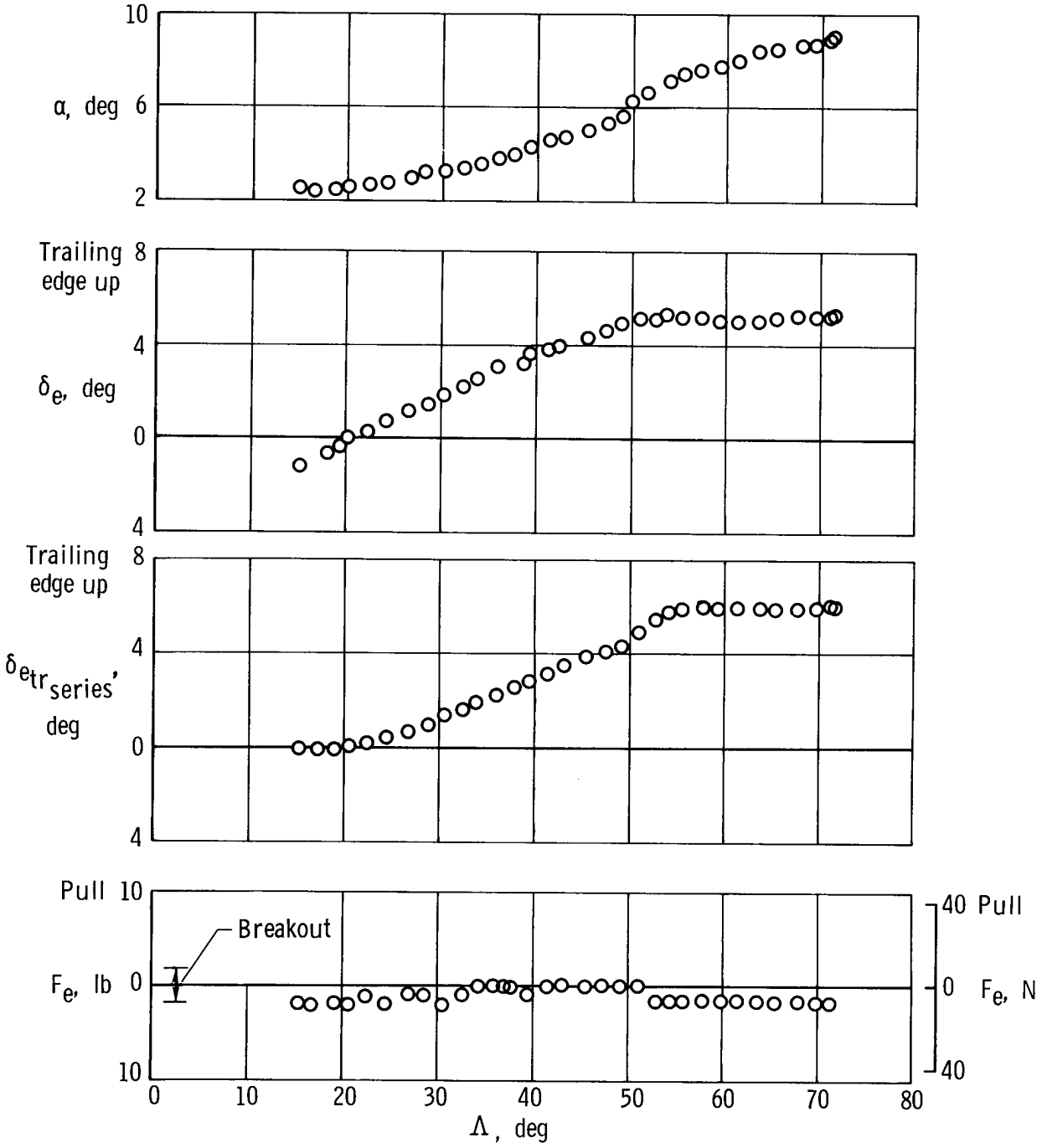

(b) Trim change with wing sweep. Clean configuration; $M_i = 0.74$; $h_{p_i} = 22,300$ ft (6797 m); gross weight = 72,000 lb (32,695 kg); variable center of gravity.

Figure 6. – Continued.

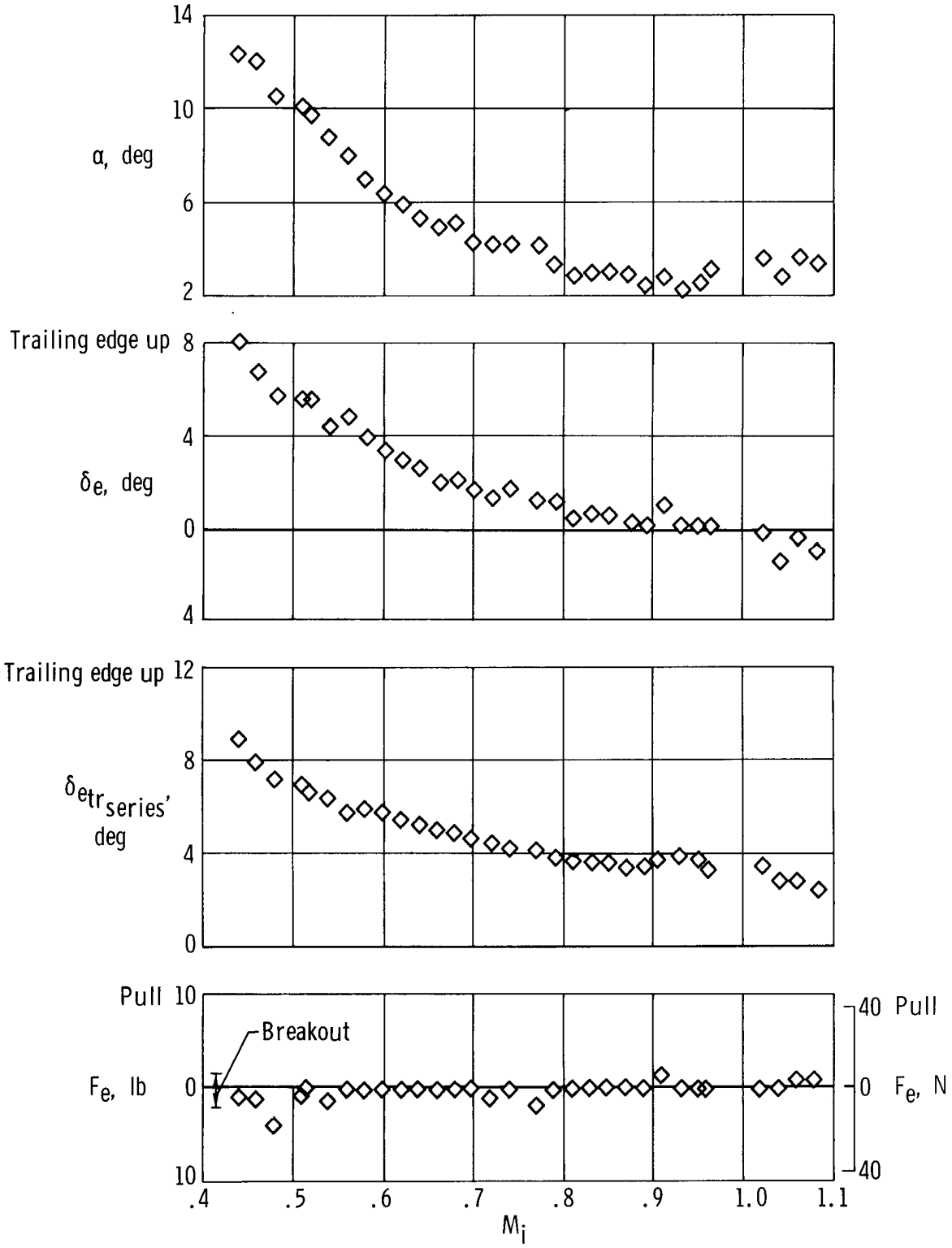

(c) Automatic trim feature during constant-altitude acceleration. $\Lambda = 50°$; $h_{p_i} = 10,000$ ft (3048 m); gross weight = 75,500 lb (34,240 kg); center of gravity = 15.5 percent.

Figure 6. – Continued.

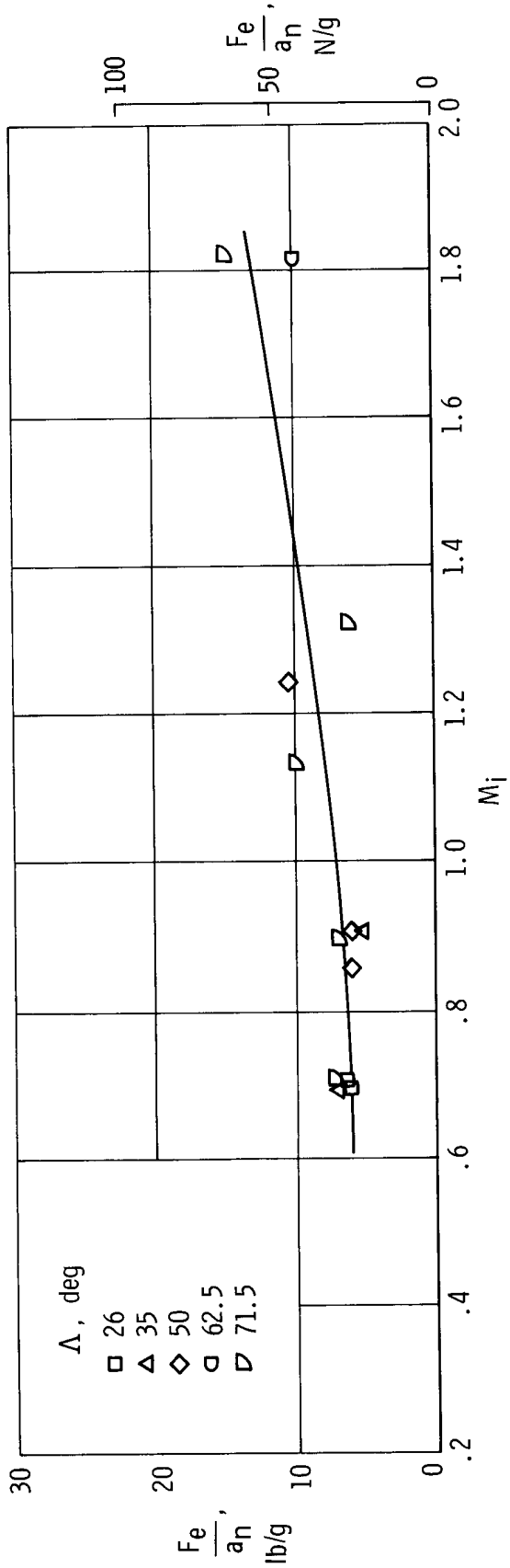

(d) Longitudinal maneuver gradient along arbitrary climb corridor of figure 5. Not corrected to constant gross weight and center of gravity.

Figure 6. – Concluded.

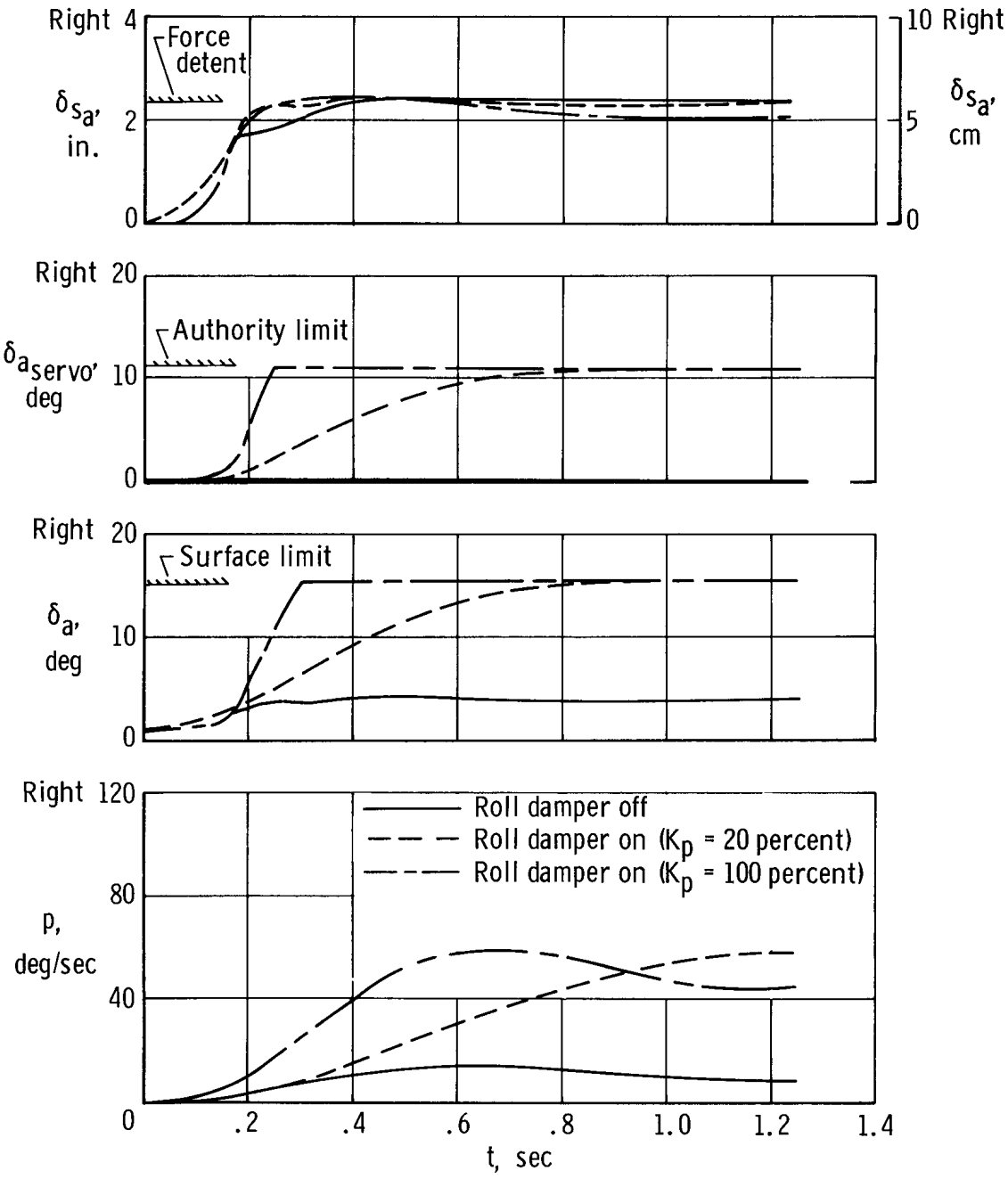

(a) Effect of roll damper and gain. $\Lambda = 50°$ (spoilers inoperative); $M_i = 0.72$; $h_{p_i} = 20,500$ ft (6248 m).

Figure 7. – F-111A lateral command augmentation characteristics.

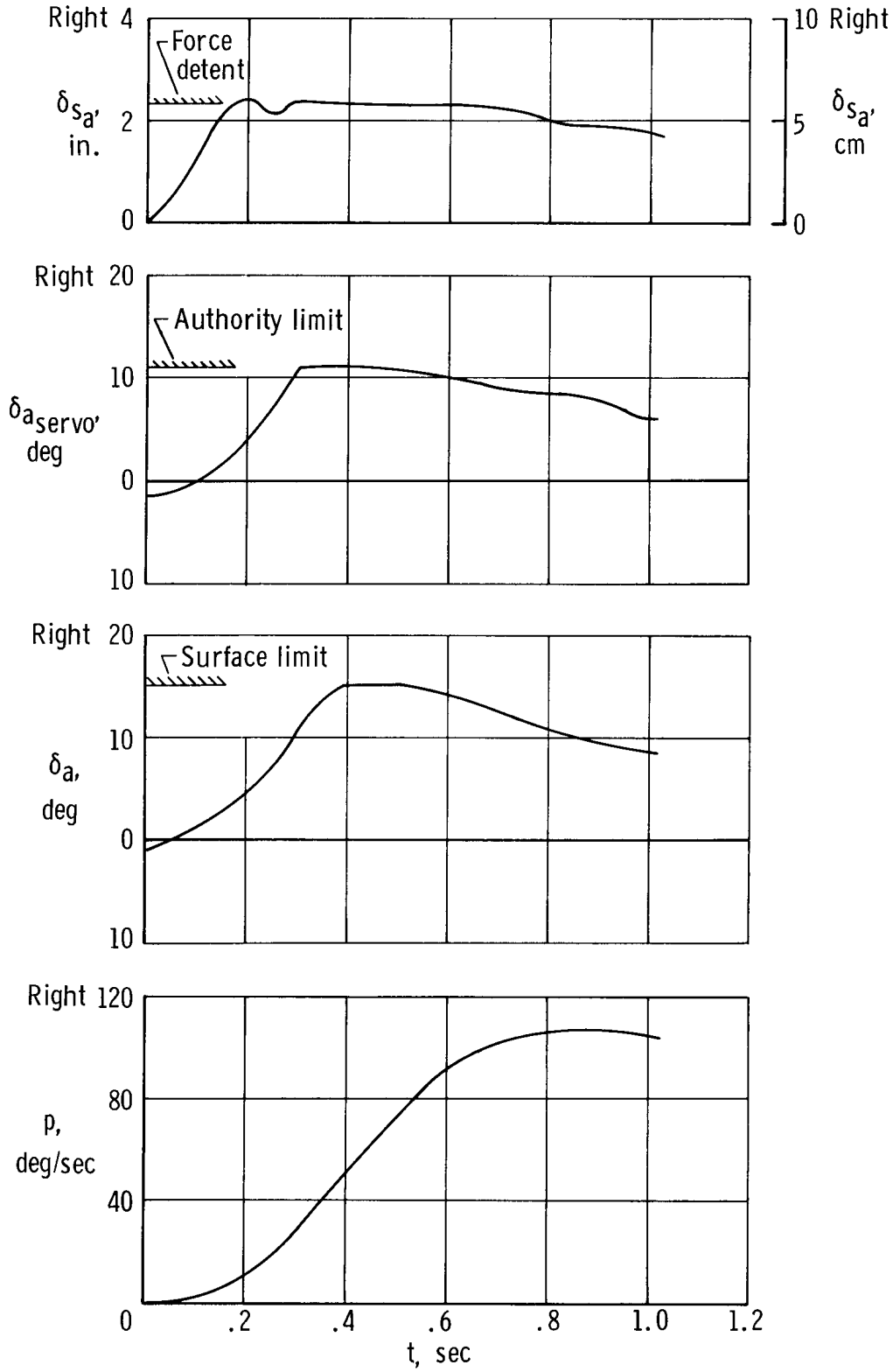

(b) Example of augmentation system characteristic. $\Lambda = 45°$ (spoilers operative); $M_i = 0.71$; $h_{p_i} = 20,100$ ft (6126 m); $K_p = 82$ percent.

Figure 7. – Concluded.

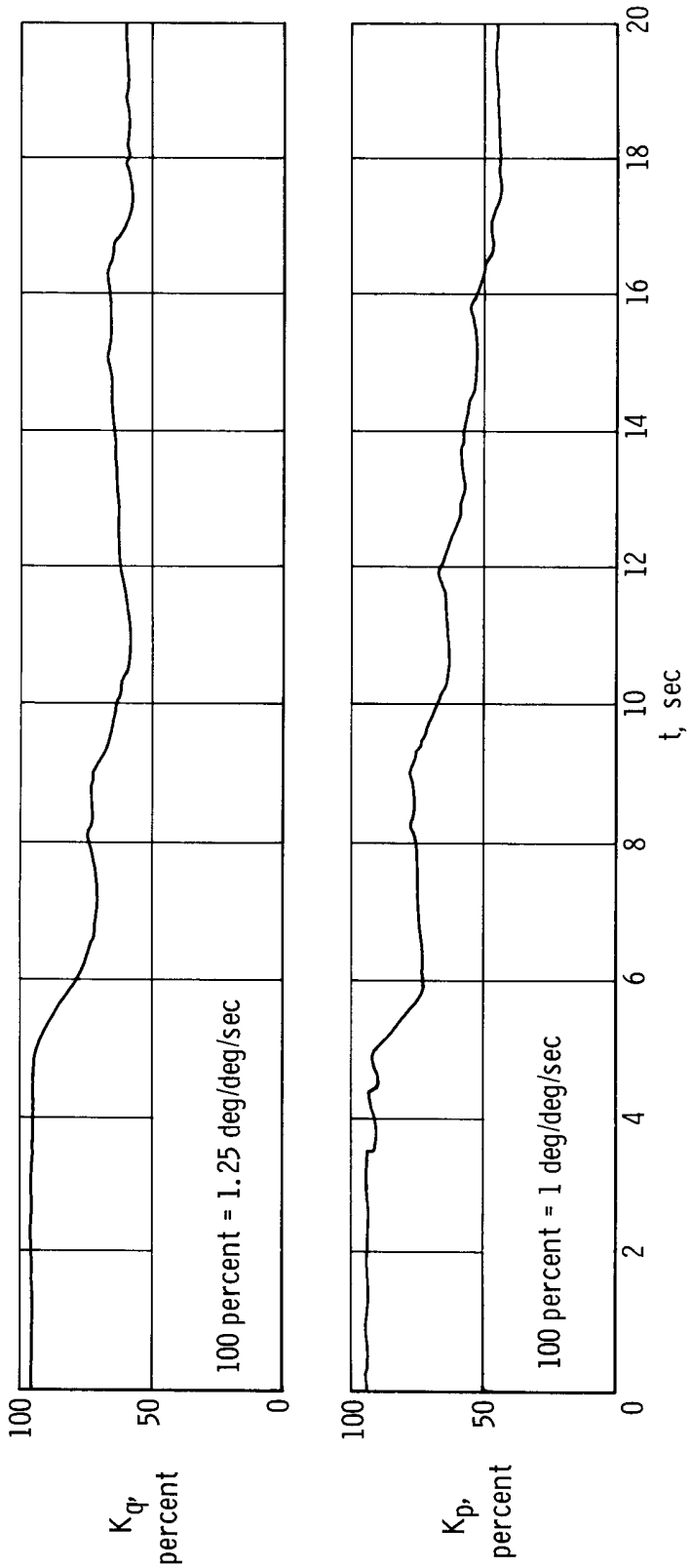

(a) Gain reduction due to buffet and light control activity. $\Lambda = 26°$; $M_i = 0.70$; $h_{p_i} = 25,000$ ft (7620 m).

Figure 8.– F-111A adaptive-gain characteristics.

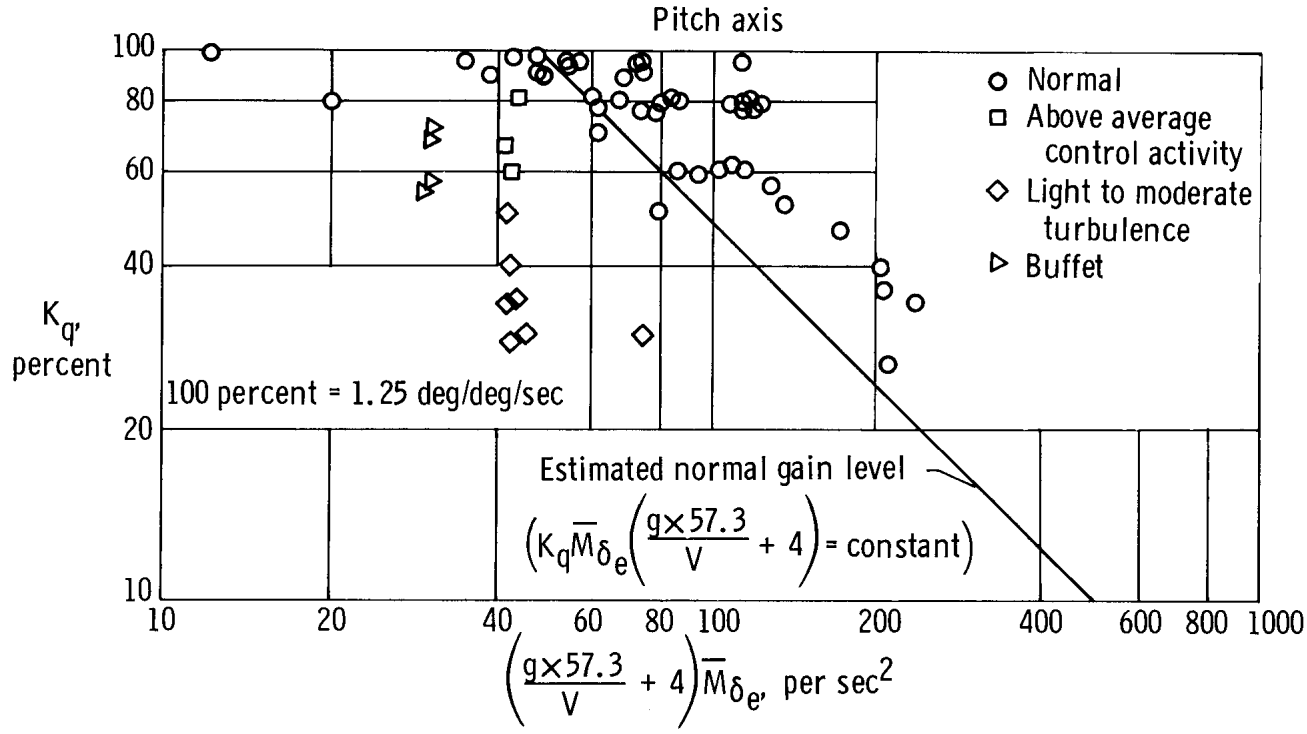

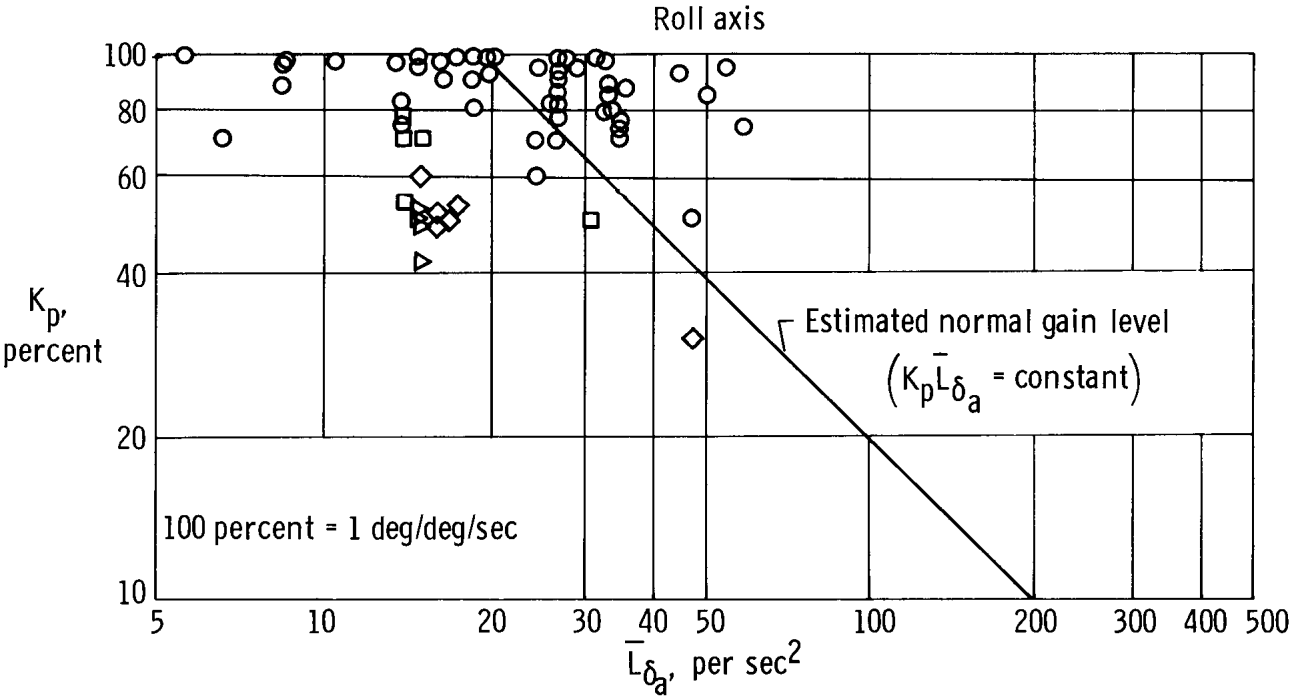

(b) Summary of gain activity ($\bar{M}_{\delta_e}$ and $\bar{L}_{\delta_a}$ from contractor's predictions).

Figure 8. – Concluded.

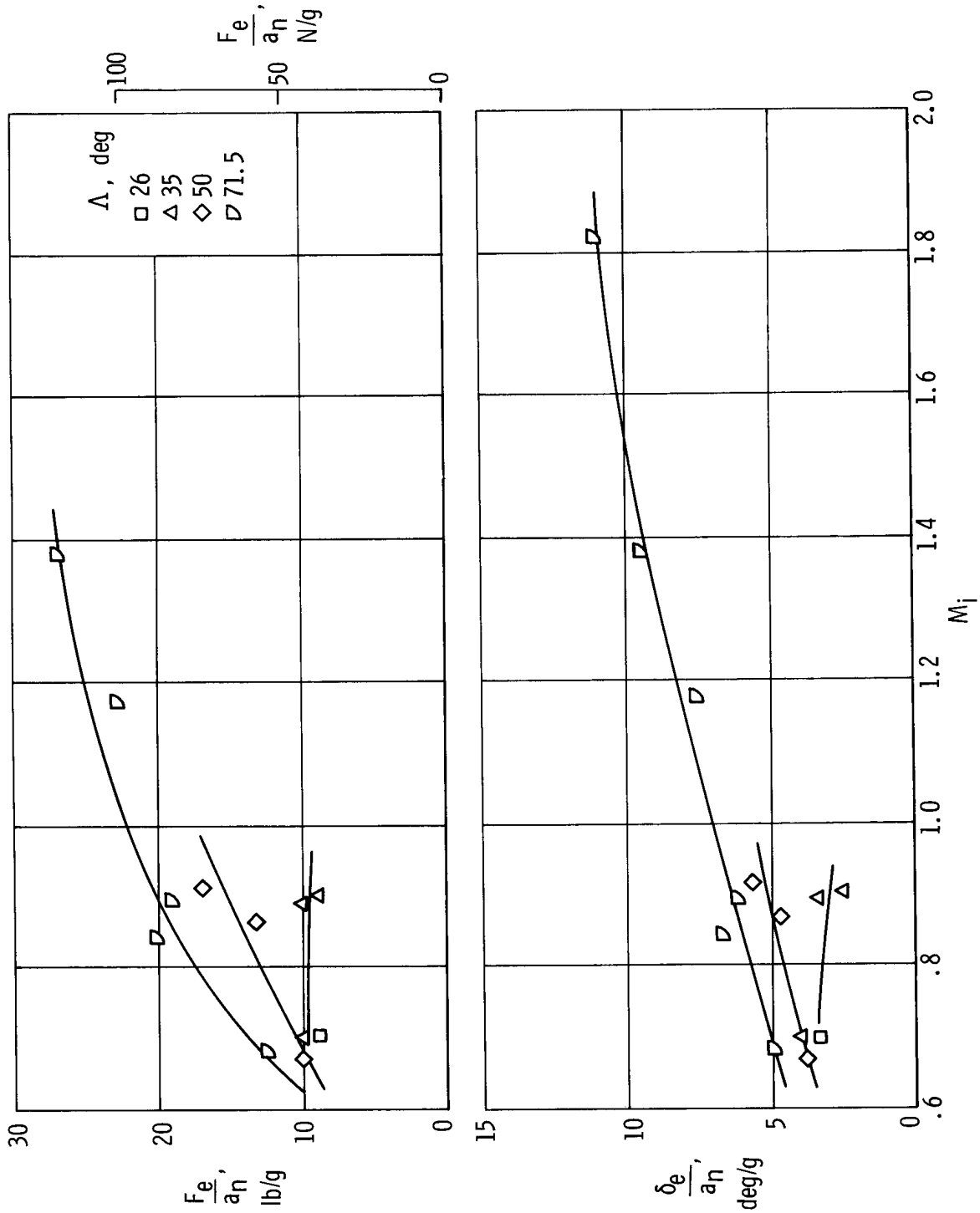

Figure 9. – F-111A longitudinal maneuver gradients along arbitrary climb corridor of figure 5 with pitch damper off. Not corrected to constant gross weight and center of gravity.

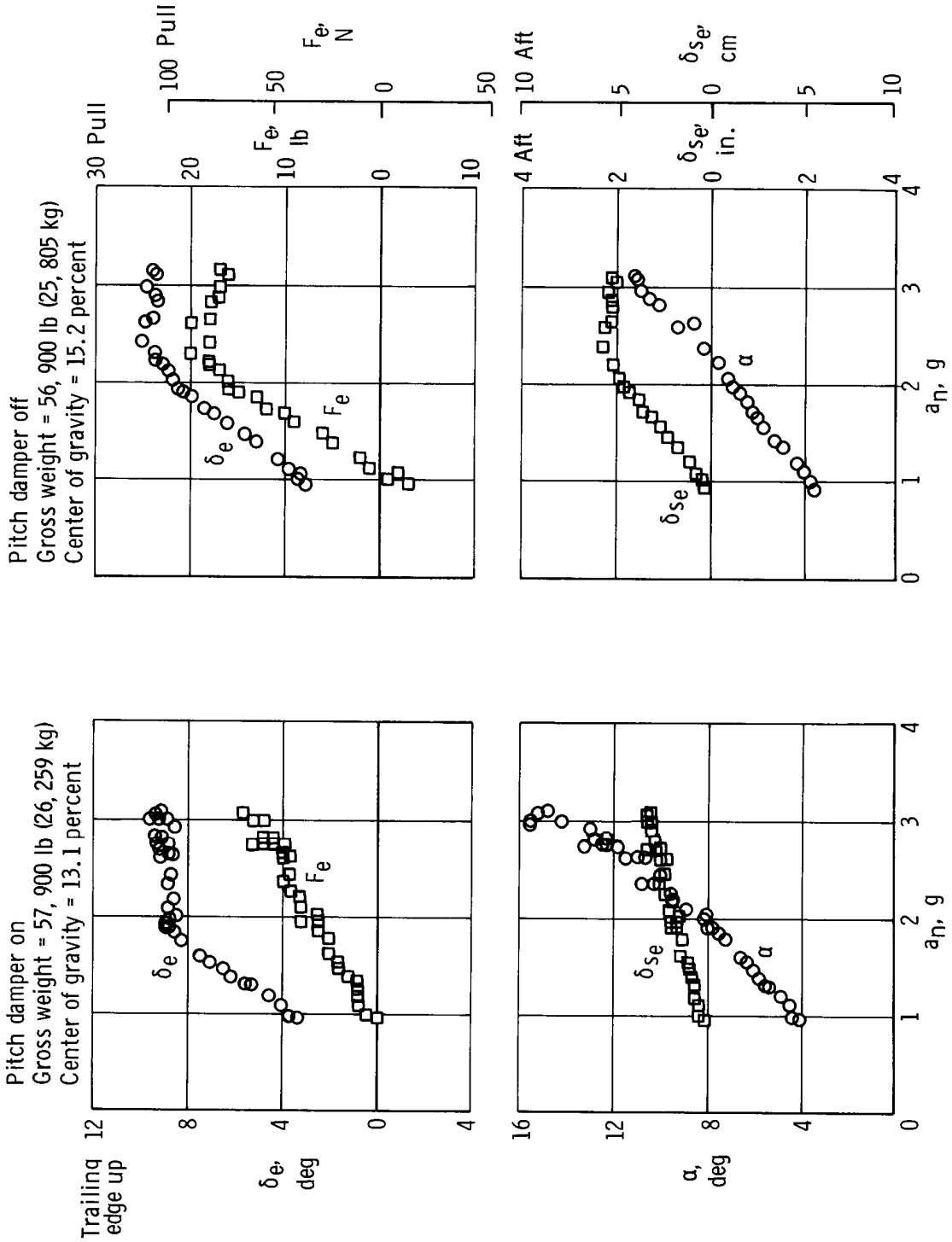

(a) Effect of pitch damper.

Figure 10. – F-111A longitudinal maneuvering characteristics illustrating pitch-up.
$\Lambda = 50°$; $M_i = 0.92$; $h_{p_i} = 28,000$ ft (8534 m).

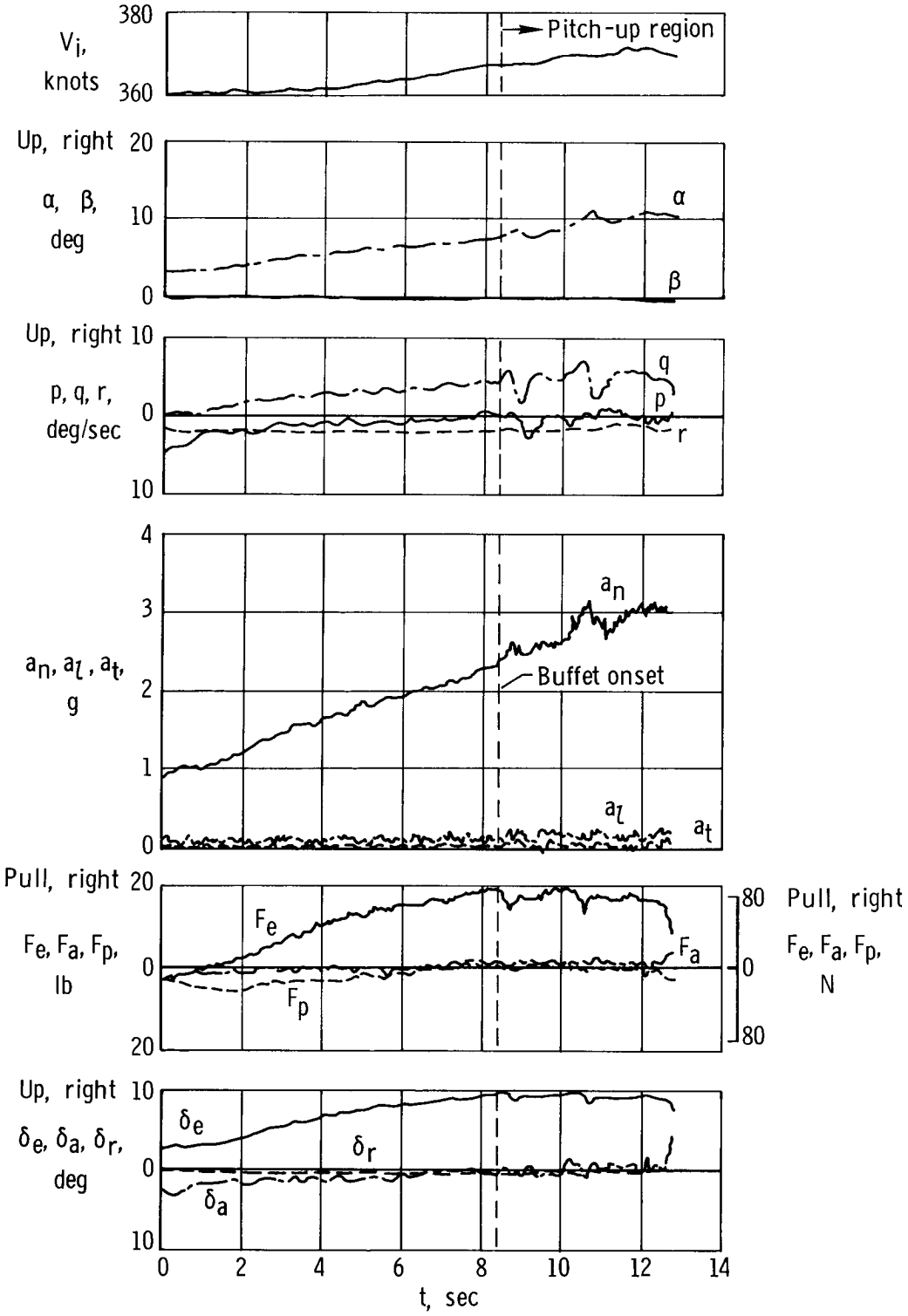

(b) Time history of longitudinal maneuver illustrating control effectiveness during pitch-up. Gross weight = 56,900 lb (25,805 kg); center of gravity = 15.2 percent; pitch damper off.

Figure 10. – Continued.

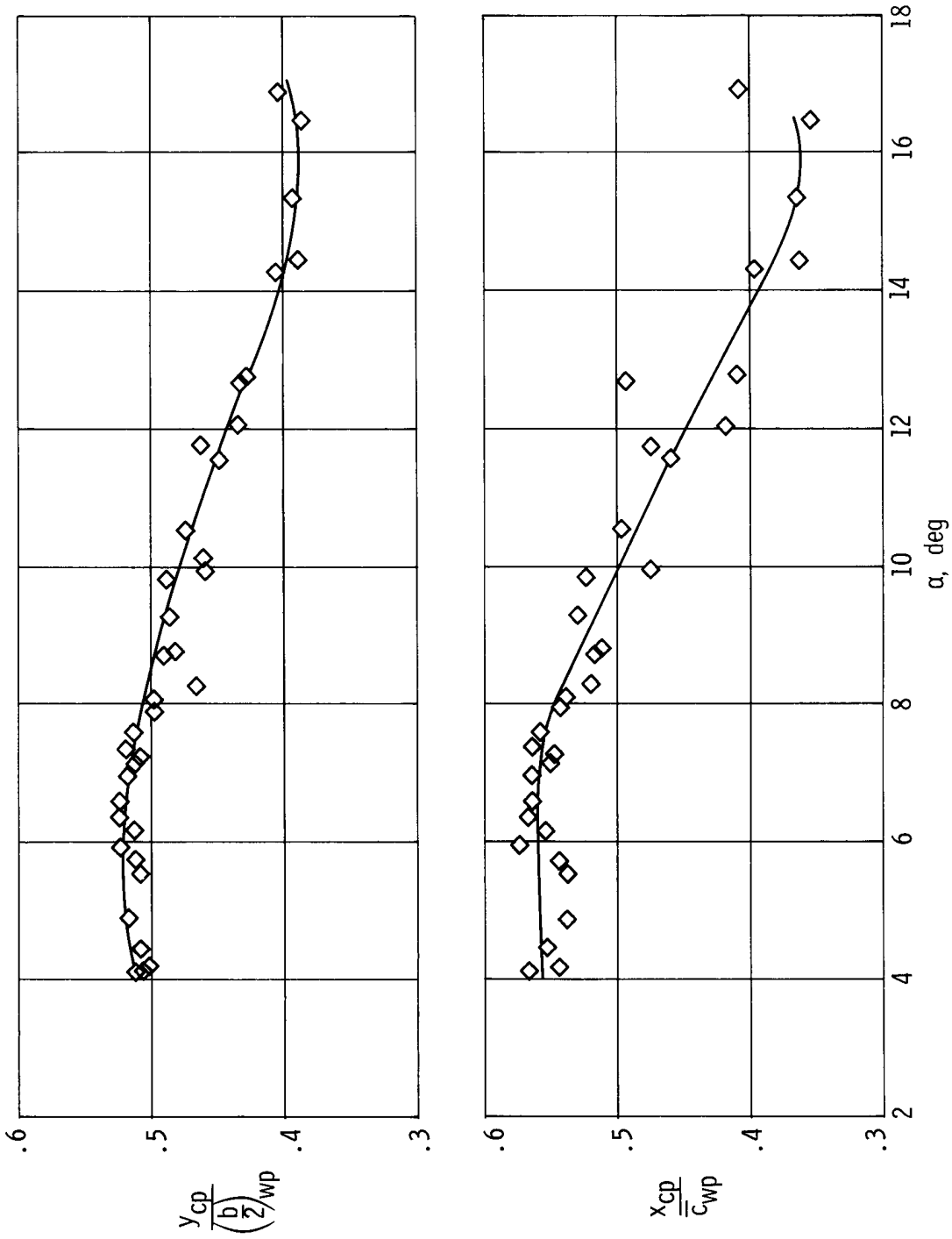

(c) Variation of wing-panel center of pressure during a longitudinal maneuver.

Figure 10. – Concluded.

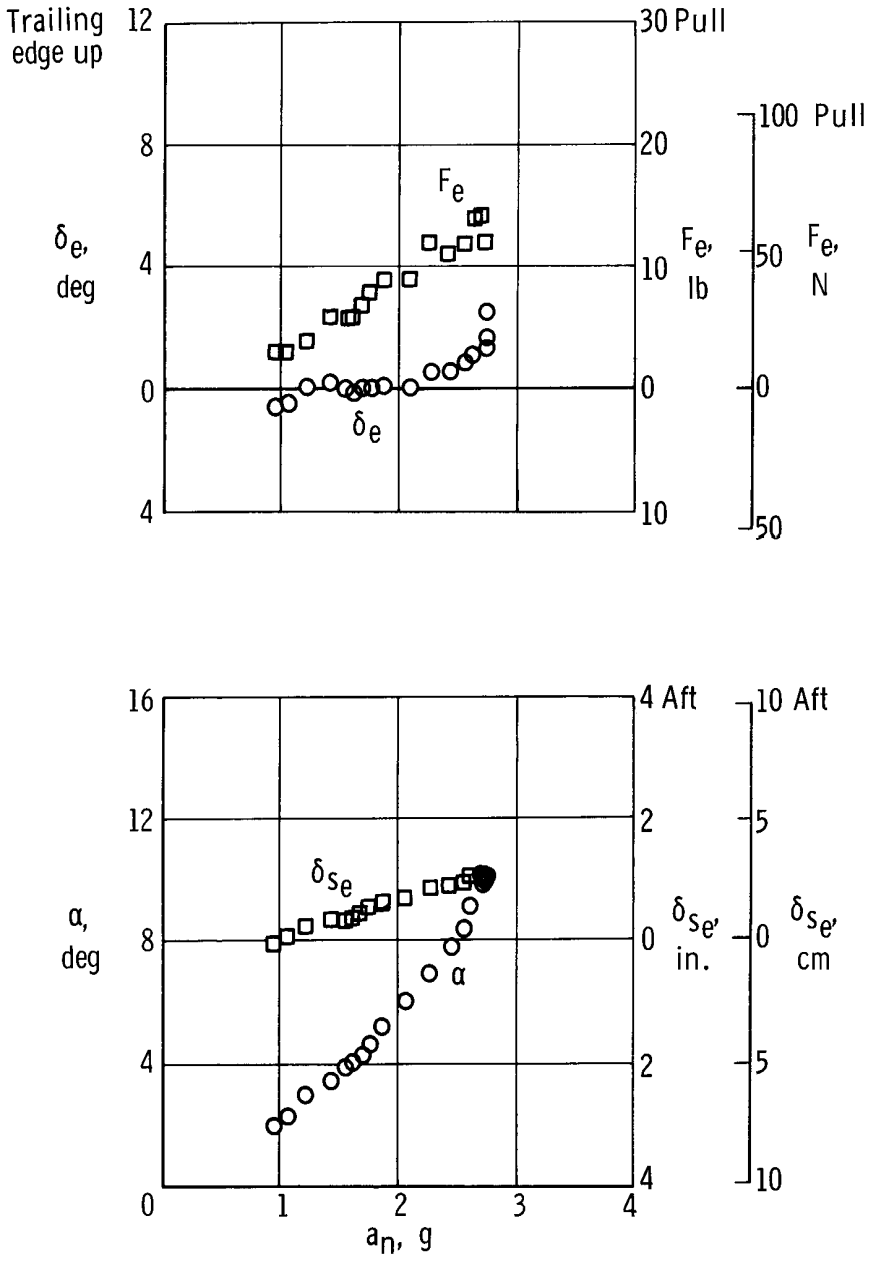

Figure 11. – F-111A longitudinal maneuvering characteristics illustrating apparent stability recovery above pitch-up. $\Lambda = 26°$; $M_i = 0.79$; $h_{p_i} = 25,700$ ft (7833 m); gross weight = 60,700 lb (27,528 kg); center of gravity = 25.0 percent; pitch damper on.

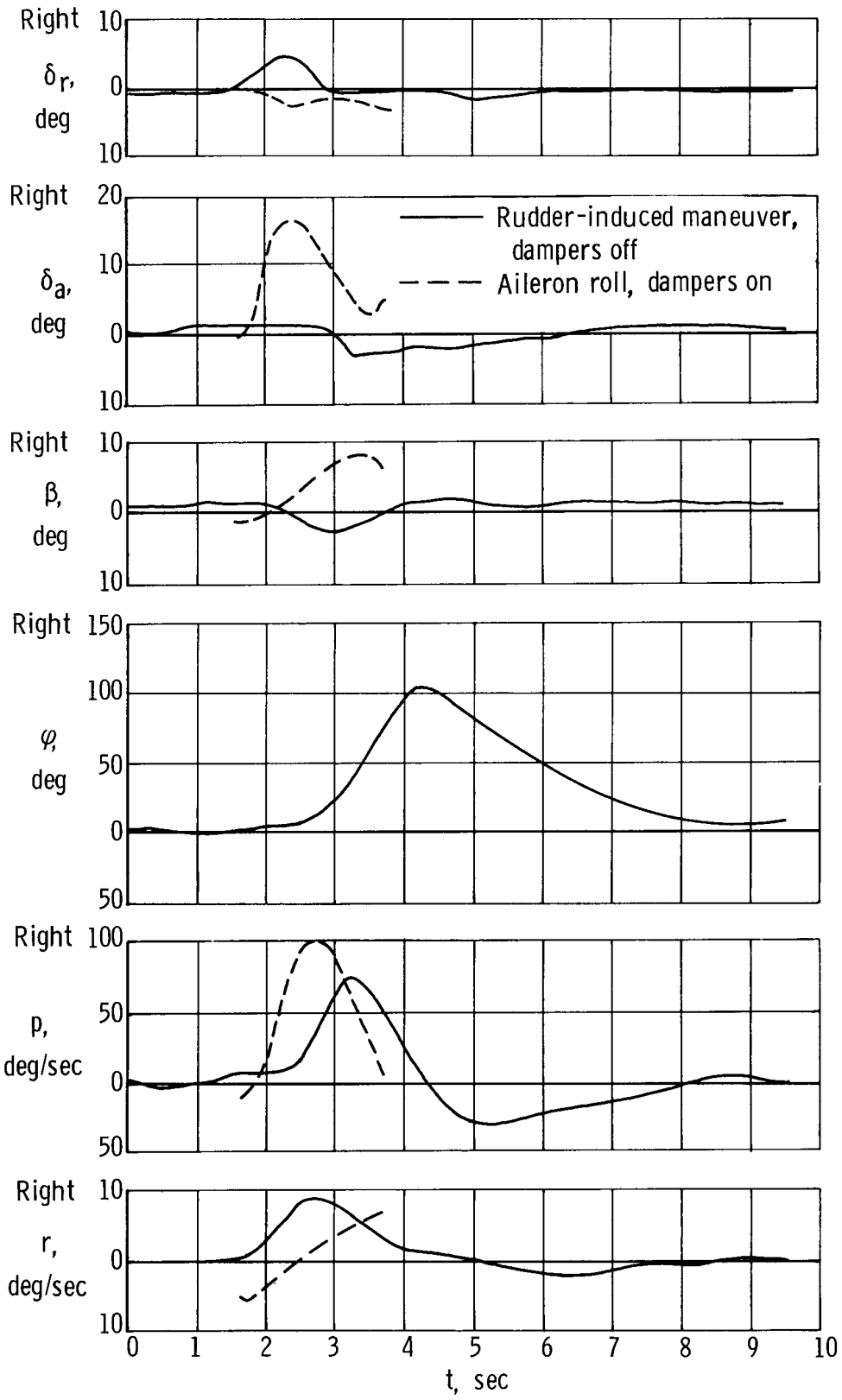

Figure 12. – Comparison of rudder-induced lateral-directional maneuver with full-deflection aileron roll for the F-111A. $\Lambda = 71.5°$; $M_i \approx 0.75$; $h_{p_i} \approx 23{,}000$ ft (7010 m).

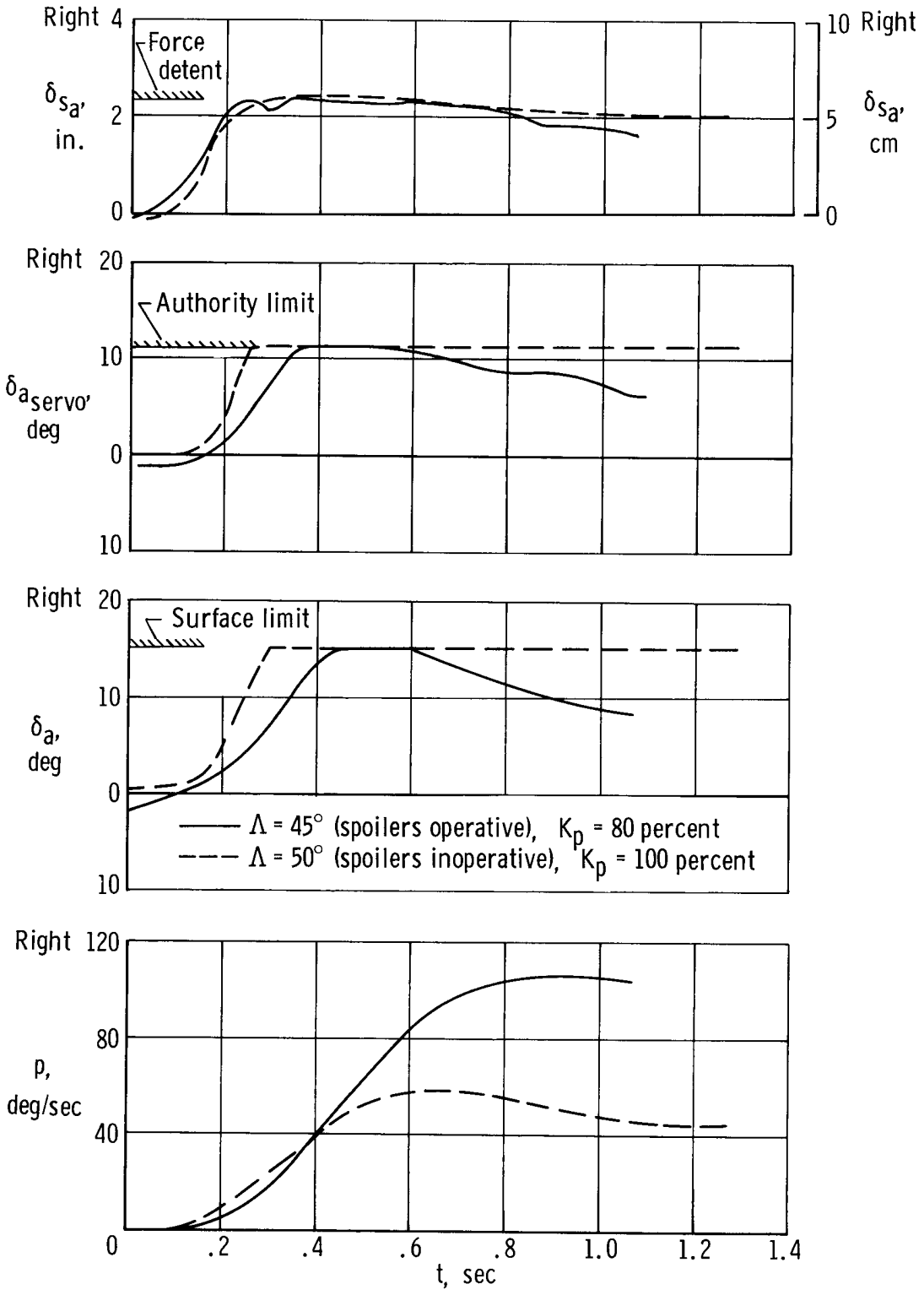

(a) Effect of spoilers.

Figure 13. – F-111A lateral maneuverability characteristics. M_i = 0.71; h_{p_i} = 20,000 ft (6096 m); dampers on.

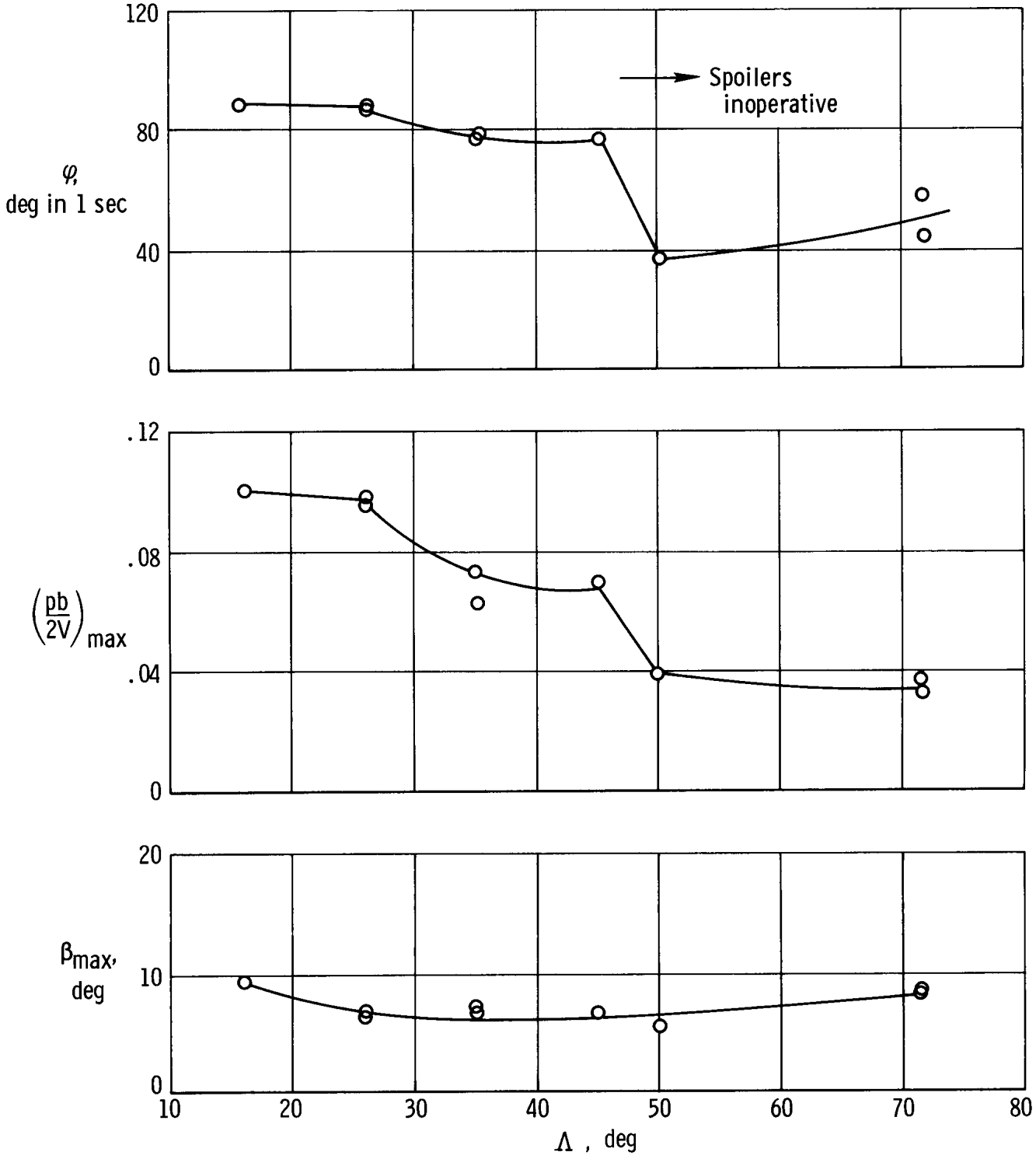

(b) Effect of wing sweep. Data adjusted to 15°δ_a or 135 deg/sec roll rate; b in $\left(\frac{pb}{2V}\right)_{max}$ based on appropriate wing sweep (see fig. 2).

Figure 13. – Concluded.

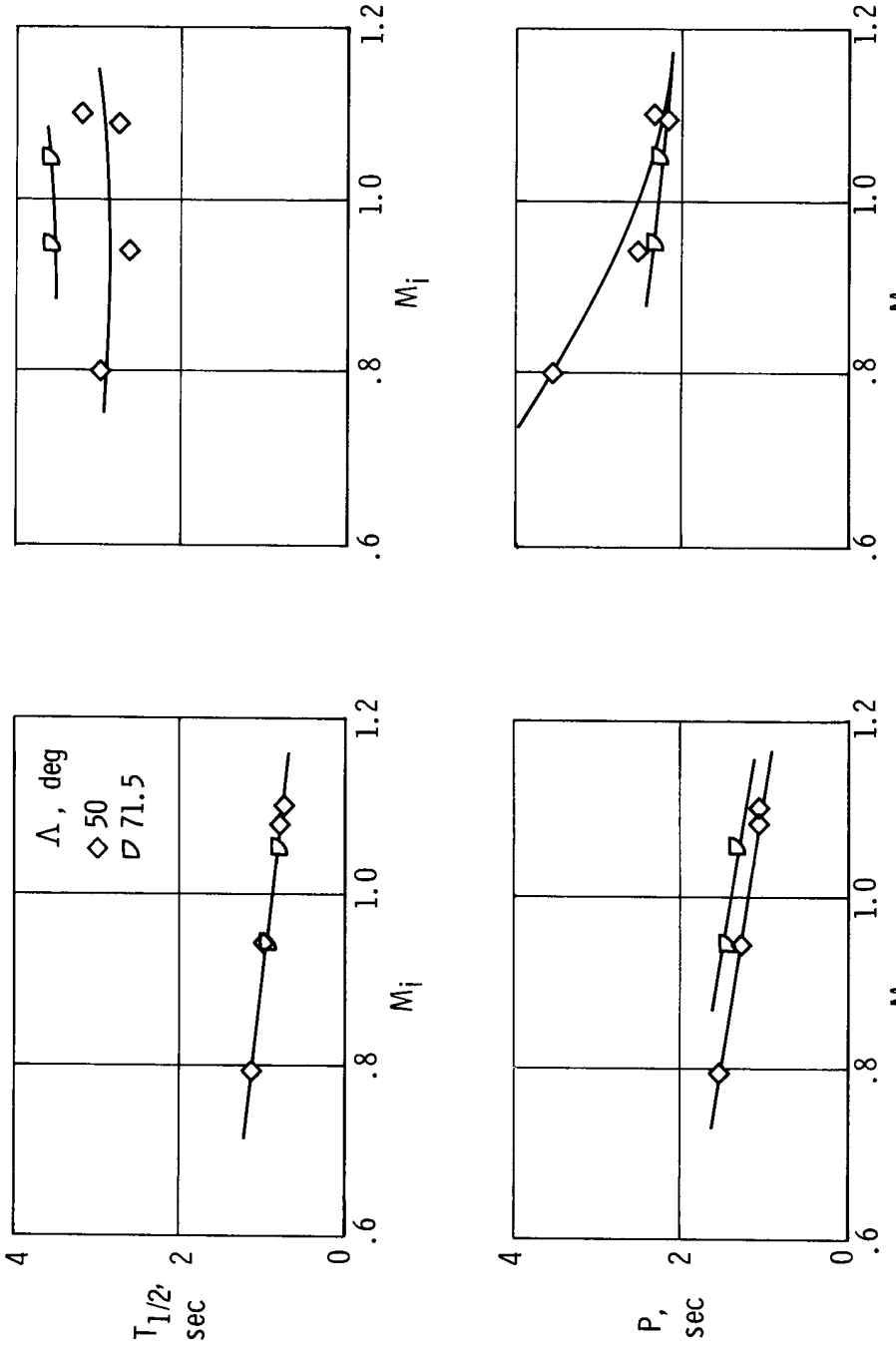

(a) Longitudinal short period.

(b) Dutch roll.

Figure 14. – F-111A unaugmented short-period dynamic characteristics at 10,000 ft (3048 m) altitude.

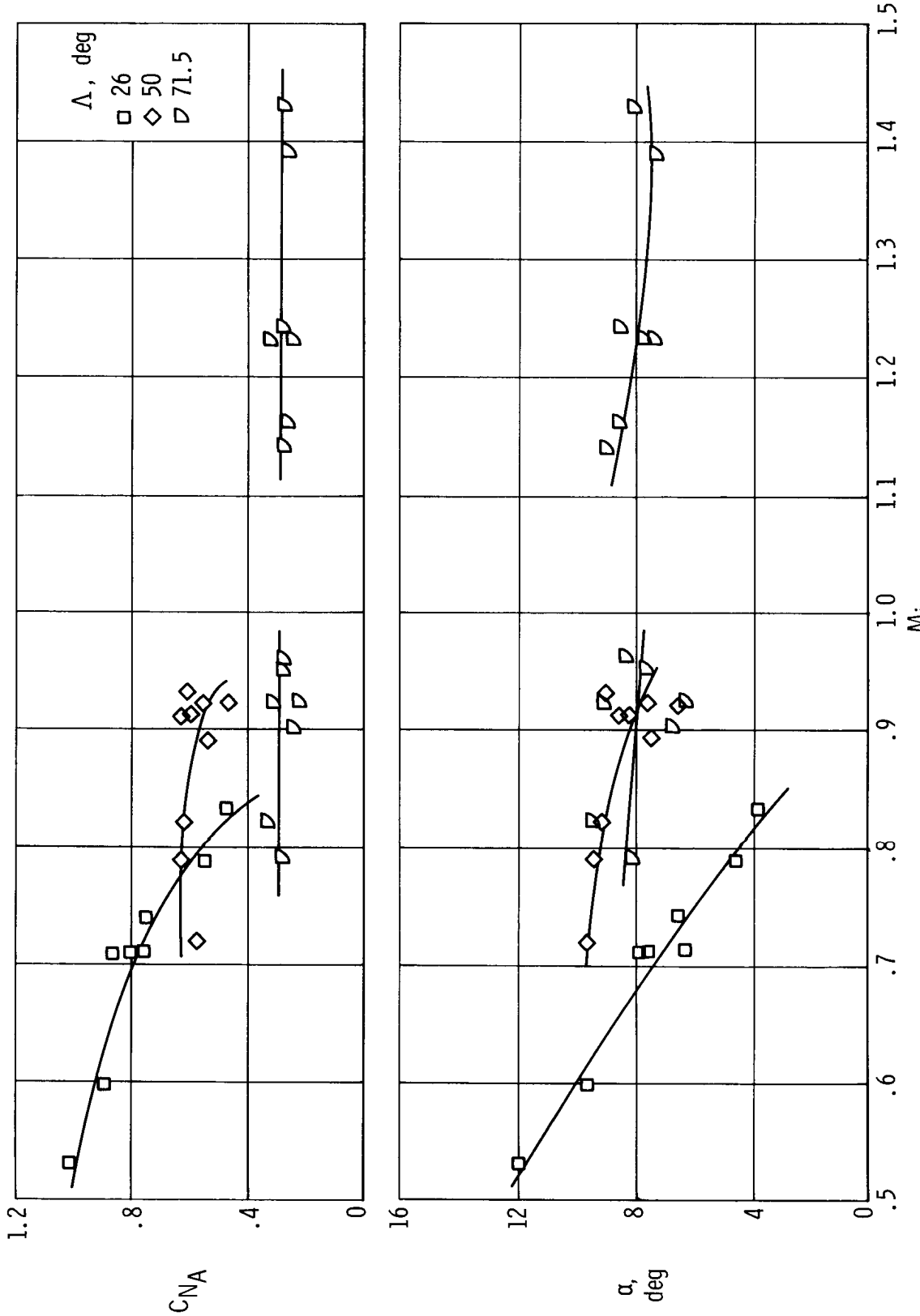

Figure 15. – Variation of airplane normal-force coefficient and angle of attack with indicated Mach number for F-111A buffet onset.

NASA-Langley, 1968 — 2